

Phase structure of lattice $SU(2) \otimes U_S(1)$ three-dimensional gauge theory

K. Farakos

National Technical University of Athens, Department of Physics, Zografou Campus 157 73, Athens, Greece

N. E. Mavromatos

University of Oxford, Department of (Theoretical) Physics, 1 Keble Road OX1 3NP, Oxford, United Kingdom

D. McNeill

University of Oxford, Department of (Theoretical) Physics, 1 Keble Road OX1 3NP, Oxford, United Kingdom

(Received 29 June 1998; published 6 January 1999)

We discuss a phase diagram for a relativistic $SU(2) \times U_S(1)$ lattice gauge theory, with emphasis on the formation of a parity-invariant chiral condensate, in the case when the $U_S(1)$ field is infinitely coupled, and the $SU(2)$ field is moved away from infinite coupling by means of a strong-coupling expansion. We provide analytical arguments on the existence of (and partially derive) a critical line in coupling space, separating the phase of broken $SU(2)$ symmetry from that where the symmetry is unbroken. We review unconventional (Kosterlitz-Thouless type) superconducting properties of the model, upon coupling it to external electromagnetic potentials. We discuss the role of instantons of the unbroken subgroup $U(1) \in SU(2)$, in eventually destroying superconductivity under certain circumstances. The model may have applications to the theory of high-temperature superconductivity. In particular, we argue that in the regime of the couplings leading to the broken $SU(2)$ phase, the model may provide an explanation on the appearance of a pseudogap phase, lying between the antiferromagnetic and the superconducting phases. In such a phase, a fermion mass gap appears in the theory, but there is no phase coherence, due to the Kosterlitz-Thouless mode of symmetry breaking. The absence of superconductivity in this phase is attributed to nonperturbative effects (instantons) of the gauge field $U(1) \in SU(2)$. [S0556-2821(99)04701-3]

PACS number(s): 11.25.Hf, 74.20.Mn

I. INTRODUCTION

There has been a great deal of recent interest in the dynamical symmetry breaking patterns of three-dimensional quantum gauge field theories, both from the pure particle theory standpoint [1–3], and as a tool for describing models of high- T_c superconductors [4–6]. The gauge theories studied in those works have been either three-dimensional QED (QED₃) and variants of it [1,4,5], or $SU(2) \otimes U(1)$ [2,6].

From the condensed-matter viewpoint, which motivated our approach to the subject, the key suggestion which lead to a non-Abelian dynamical gauge symmetry structure for the doped antiferromagnet, was the *slave-fermion* spin-charge separation ansatz for physical electron operators at *each lattice site* i [6]:

$$\begin{aligned} \chi_{\alpha\beta,i} &\equiv \begin{pmatrix} c_1 & c_2 \\ c_2^\dagger & -c_1^\dagger \end{pmatrix}_i \equiv \hat{\psi}_{\alpha\gamma,i} \hat{z}_{\gamma\beta,i} \\ &= \begin{pmatrix} \psi_1 & \psi_2 \\ -\psi_2^\dagger & \psi_1^\dagger \end{pmatrix}_i \begin{pmatrix} z_1 & -\bar{z}_2 \\ z_2 & \bar{z}_1 \end{pmatrix}_i, \end{aligned} \quad (1)$$

where $\chi_{\alpha\beta}$ are ‘‘particle-hole’’ matrix-valued operators [7], c_α , $\alpha=1,2$ are electron annihilation operators, the Grassmann variables ψ_i , $i=1,2$ play the role of holon excitations, while the bosonic fields z_i , $i=1,2$, represent magnon excitations [8]. The ansatz (1) has spin-electric-charge separation, since only the fields ψ_i carry *electric* charge. The holon

fields $\hat{\psi}_{\alpha\beta}$ may be viewed as substructures of the physical electron $\chi_{\alpha\beta}$ [9], in close analogy to the ‘‘quarks’’ of QCD.

As argued in Ref. [6] the ansatz is characterized by the following *local* phase (gauge) symmetry structure:

$$G = SU(2) \times U_S(1) \times U_E(1). \quad (2)$$

The $U_E(1)$ electromagnetic symmetry is due to the electric charge of the holons. In the absence of external electromagnetic potentials is a global symmetry (fermion number). It becomes local (gauged) after coupling to external electromagnetism.

The local $SU(2)$ symmetry is discovered if one defines the transformation properties of the $\hat{z}_{\alpha\beta}$ and $\hat{\psi}_{\alpha\beta}^\dagger$ fields to be given by left multiplication with the $SU(2)$ matrices, and pertains to the spin degrees of freedom. The local $U_S(1)$ ‘‘statistical’’ phase symmetry allows fractional statistics of the spin and charge excitations. This is an exclusive feature of the three dimensional geometry, and is similar in spirit to the bosonization technique of the spin-charge separation ansatz of Ref. [10]. The presence of $U_S(1)$ allows the alternative possibility of representing the holes as slave bosons and the spin excitations as fermions.

In the model of Ref. [6], this $U_S(1)$ is assumed strongly coupled, capable of holon $\hat{\psi}$ pairing and (parity-preserving) mass-gap generation. The mass generation breaks chiral symmetry, which can be defined in three-dimensional theories with *even* number of fermion species [1], as is the case of the model of Ref. [6]. However, as discussed in Refs.

[11,4,6], this mass gap is not accompanied by any phase coherence, given that the symmetry breaking is realized in the Kosterlitz-Thouless mode [12].

At this stage we would like to make an important comment, concerning the *relativistic nature* of the effective model discussed in Ref. [6]. From a condensed-matter view point, such relativistic systems would arise by a *linearization about specific points on the fermi surface* of the statistical system, such as nodes, etc. In this respect it is worthy of mentioning that recent experimental tests [13] imply that the superconducting gap in the high- T_c cuprates is of d -wave type, with lines of nodes on the fermi surface. It is the linearization about such nodes, in the flux phase for the $U_S(1)$ gauge field, that leads to Dirac spectrum for holon excitations, with the fermi velocity of holes playing the role of the limiting (“light”) velocity, as suggested above and in Refs. [4,6]. Then, as a result of the Kosterlitz-Thouless (KT) mechanism for superconductivity described in Ref. [4,6], a fermion gap opens at those nodes, which, due to the absence of a local-order parameter, respects the d -wave character of the superconducting state.

The pertinent long-wavelength lattice gauge model, describing the low-energy dynamics around such d -wave nodes, assumes the form [6]

$$H_{HF} = \sum_{\langle ij \rangle} \text{tr} \{ (8/J) \Delta_{ij}^\dagger \Delta_{ji} + \hat{K} [-t_{ij}(1 + \sigma_3) + \Delta_{ij}] \times \hat{\psi}_j V_{ji} U_{ji} \hat{\psi}_i^\dagger \} + \sum_{\langle ij \rangle} \text{tr} [\hat{K} \hat{z}_i V_{ij} U_{ij} \hat{z}_j] + \text{H.c.}, \quad (3)$$

where J is the Heisenberg antiferromagnetic interaction, \hat{K} is a normalization constant, Δ_{ij} is a Hubbard-Stratonovich field that linearizes four-electron interaction terms in the original Hubbard model, and U_{ij}, V_{ij} are the link variables for the $U_S(1)$ and $SU(2)$ groups, respectively. The conventional lattice gauge theory form of the action (3) is derived upon freezing the fluctuations of the Δ_{ij} field [6], and integrating out the (massive) magnon fields z in the path integral. This latter operation yields appropriate Maxwell kinetic terms for the link variables V_{ij}, U_{ij} , in a low-energy derivative expansion [5,14]. On the lattice such kinetic terms are given by plaquette terms of the form [6]

$$\sum_p [\beta_{SU(2)} (1 - \text{Tr } V_p) + \beta_{U_S(1)} (1 - \text{Tr } U_p)], \quad (4)$$

where p denotes sum over plaquettes of the lattice, and $\beta_{U_S(1)} \equiv \beta_1, \beta_{SU(2)} \equiv \beta_2 = 4\beta_1$ are the dimensionless (in units of the lattice spacing) inverse square couplings of the $U_S(1)$ and $SU(2)$ groups, respectively [6]. The above relation between the β_i 's is due to the specific form of the z -dependent terms in Eq. (3), which results in the same induced couplings $g_{SU(2)}^2 = g_{U_S(1)}^2$. Moreover, there is a non-trivial connection of the gauge group couplings to \hat{K} [6]:

$$\hat{K} \propto g_{SU(2)}^2 = g_{U_S(1)}^2 \sim J \eta \quad (5)$$

with $\eta = 1 - \delta$, δ being the doping concentration in the sample [6,15]. To cast the symmetry structure in a form that is familiar to particle physicists, one may change representation of the $SU(2)$ group, and instead of working with 2×2 matrices in Eq. (1), one may use a representation in which the fermionic matrices $\hat{\psi}_{\alpha\beta}$ are represented as two-component (Dirac) spinors in “color” space:

$$\tilde{\Psi}_{1,i}^\dagger = (\psi_1 \quad -\psi_2^\dagger)_i, \quad \tilde{\Psi}_{2,i}^\dagger = (\psi_2 \quad \psi_1^\dagger)_i, \quad i = \text{lattice site}. \quad (6)$$

In this representation the two-component spinors $\tilde{\Psi}$ (6) will act as *Dirac spinors on the lattice*, and the γ -matrix (space-time) structure will be spanned by the irreducible 2×2 Dirac representation. By assuming a background $U_S(1)$ field of flux π per lattice plaquette [4], and considering quantum fluctuations around this background for the $U_S(1)$ gauge field, one can show that there is a Dirac-like structure in the fermion spectrum [16,17,4,15], which leads to a conventional Lattice gauge theory form for the effective low-energy Hamiltonian of the large- U , doped Hubbard model [6].

In the above context, a strongly coupled $U_S(1)$ group can dynamically generate a mass gap in the holon spectrum [6], which breaks the $SU(2)$ local symmetry down to its Abelian subgroup $U(1)$ generated by the σ_3 matrix. From the view point of the statistical model (3), the breaking of the $SU(2)$ symmetry down to its Abelian σ_3 subgroup may be interpreted as restricting the holon hopping effectively to a single sublattice, since the intrasublattice hopping is suppressed by the mass of the gauge bosons. In a low-energy effective theory of the massless degrees of freedom this reproduces the results of Refs. [4,18], derived under a large-spin approximation for the antiferromagnet $S \rightarrow \infty$ which is not necessary in the present approach.

The Kosterlitz-Thouless (KT) nature [12] of the $U_S(1)$ induced mass gap (absence of local order parameter), is a characteristic feature of gauge theories in $2+1$ dimensions, as argued in Refs. [11,4]. When applied to our non-Abelian model [6] it leads to unconventional KT superconductivity, provided the gauge boson of the unbroken $U(1) \in SU(2)$ is massless. Due to the compactness of the $U(1)$ gauge group, however, which is a distinctive feature of the non-Abelian gauge group nature of the spin-charge separation (1), there are nonperturbative effects (instantons), which are responsible for giving the gauge boson $U(1)$ a small but finite mass [19]. This spoils superconductivity, leaving only a phase, characterized by pairing among the holons, without the existence of phase coherence. It is one of the points of this article to argue that such a phase may provide a possible explanation of the so-called “pseudogap” phase of high-temperature superconductivity [20], an intermediate nonsuperconducting phase, lying between the antiferromagnetic and d -wave superconducting [13] phases. A preliminary discussion on this issue appeared in Ref. [21].

At this point, we would like to mention that other authors have also used relativistic fermions to describe the underdoped or pseudo-gap phase of high- T_c materials [22,23]. Their approaches, however, are different from ours: In Ref.

[22], relativistic charge excitations are used as in our model [6]. Their relativistic nature is due to the adopted scenario that the fermi surface of the underdoped cuprates consists of four small pockets, centered around $(\pm \pi/2, \pm \pi/2)$ in momentum space. However, the low-energy model used in that work, and the nature of the gauge symmetries involved, are different from our model. In the ‘‘nodal liquid’’ approach of Ref. [23], on the other hand, the relativistic Dirac-fermion excitations around the four nodes of the putative fermi surface in the underdoped situation are neutral, and, hence, from our point of view they correspond to spin degrees of freedom rather than holons. This leads to a different physical scenario for the pseudogap phase than the one discussed here and in Ref. [21].

In this article we shall discuss in some detail the phase structure of the $SU(2) \otimes U_5(1)$ gauge theory. Despite the above motivation from condensed-matter physics, the analysis and the techniques used will be those of particle physics, thereby making the results even applicable to particle physics applications of three-dimensional gauge theories, such as early universe studies, or high-temperature field theories. In this respect we mention the work by Volovik [24], which pursues the analogy between the physics of superfluid helium and that of the early universe, in an attempt to suggest condensed-matter experiments that could shed light in the physics of an early stage of our Universe. We hope that our work in this article will serve the purpose of pointing out yet another condensed-matter example, that of high-temperature superconductors, which may be connected to particle physics.

The structure of the article is as follows. In Sec. II we review the basic symmetry properties of the lattice action, including a discussion on the issue of spontaneous and/or dynamical breaking of parity in the context of the applicability of the Vafa-Witten [25] theorem on the lattice. In Sec. III we derive part of the phase diagram of the $SU(2) \otimes U_5(1)$ model, in the strong-coupling regime of the $SU(2)$ gauge group. The analysis is a nontrivial application of standard lattice strong-coupling expansions [26,27] to our model. In Sec. IV we review briefly the *unconventional* superconducting properties of the system upon coupling it to external electromagnetic fields. Emphasis is placed on the Kosterlitz-Thouless type of breaking of the electromagnetic symmetry, which is not accompanied by phase coherence. In Sec. V we discuss briefly the role of instantons in destroying superconductivity, but maintaining pairing and fermion gap formation. In Sec. VI we discuss a possible application of the model to the physics of high-temperature superconductors, with emphasis on the abovementioned role of instantons in inducing a pseudogap phase. This is an exclusive feature of the non-Abelian model of Ref. [6]. The possibility of tuning the doping concentration in the sample to reach supersymmetric points in coupling-constant space [28], with interesting consequences, is also mentioned briefly. Moreover, the role of additional four-fermion interactions, which may dominate the superconducting phase, is pointed out. Conclusions and outlook are presented in Sec. VII. Some technical aspects of our approach, such as rules of strong-coupling

expansion, and the evaluation of a Jacobian in the transition from fermionic lattice variables to mesonic fields, are given in three Appendices.

II. BASIC SYMMETRY STRUCTURE OF THE $SU(2) \otimes U_5(1)$ THEORY

A. The Lagrangian of the model and its symmetries

The theory (3) corresponds, after integrating out the magnon degrees of freedom z [6], to a (low-energy) lattice Lagrangian given by [2,29]

$$S[\bar{\Psi}, \Psi, V, U] = \frac{K}{2} \sum_{i,\mu} [\bar{\Psi}_i(-\gamma_\mu) U_{i,\mu} V_{i,\mu} \Psi_{i+\mu} + \bar{\Psi}_{i+\mu}(\gamma_\mu) U_{i,\mu}^\dagger V_{i,\mu}^\dagger \Psi_i] + \beta_1 \sum_p (1 - \text{tr } U_p) + \beta_2 \sum_p (1 - \text{tr } V_p), \quad (7)$$

where $U_{i,\mu} = \exp(i\theta_{i,\mu})$ represents the statistical $U_5(1)$ gauge field and $V_{i,\mu} = \exp(i\sigma^a B_a)$ is the $SU(2)$ gauge field. The quantity $K \equiv \hat{K}|t_{ij}|$, with $|t_{ij}| = t$ assumed small [6]. The fermions are 2 component spinors in *both* Dirac (Greek) and color (Latin) space $\Psi \equiv \Psi_a^\alpha$ and the generators of the $SU(2)$ group are the 2×2 Pauli matrices σ_i^{ab} , $i=1,2,3$. The Dirac matrices can also be taken to have the Pauli matrix representation [we continue to write them as $\gamma_\mu^{\alpha\beta}$, to distinguish them from the $SU(2)$ color matrices]. Here we have passed onto a three-dimensional Euclidean lattice formalism, in which $\bar{\Psi}$ is identified with Ψ^\dagger . For completeness we mention that the (naive) continuum Lagrangian corresponding to Eq. (7) is given by

$$\mathcal{L} = -\frac{1}{4}(F_{\mu\nu})^2 - \frac{1}{4}(\mathcal{G}_{\mu\nu})^2 + \bar{\Psi} D_\mu \gamma_\mu \Psi, \quad (8)$$

where $D_\mu = \partial_\mu - ig_1 a_\mu^S - ig_2 \sigma^a B_{a,\mu}$, and $F_{\mu\nu}, \mathcal{G}_{\mu\nu}$ represent the field strengths for the $U_5(1), SU(2)$ gauge groups, respectively.

There are two sets of bilinears which transform as triplets under a $SU(2)$ transformation:

$$\mathcal{A}_1 \equiv -i[\bar{\Psi}_1 \Psi_2 - \bar{\Psi}_2 \Psi_1], \quad \mathcal{A}_2 \equiv i[\bar{\Psi}_1 \Psi_2 + \bar{\Psi}_2 \Psi_1],$$

$$\mathcal{A}_3 \equiv \bar{\Psi}_1 \Psi_1 - \bar{\Psi}_2 \Psi_2, \quad \mathcal{F}_{1\mu} \equiv \bar{\Psi}_1 \sigma_\mu \Psi_2 + \bar{\Psi}_2 \sigma_\mu \Psi_1,$$

$$\mathcal{F}_{2\mu} \equiv i[\bar{\Psi}_1 \sigma_\mu \Psi_2 - \bar{\Psi}_2 \sigma_\mu \Psi_1],$$

$$\mathcal{F}_{3\mu} \equiv \bar{\Psi}_1 \sigma_\mu \Psi_1 - \bar{\Psi}_2 \sigma_\mu \Psi_2, \quad (9)$$

where $\bar{\Psi}_a \equiv \Psi_a^\dagger \gamma_0^{\alpha\beta}$ and two $SU(2)$ bilinear singlets given by

$$\begin{aligned} \mathcal{A}_4 &\equiv \bar{\Psi}_1 \Psi_1 + \bar{\Psi}_2 \Psi_2, & \mathcal{F}_{4,\mu} &\equiv \bar{\Psi}_1 \sigma_\mu \Psi_1 + \bar{\Psi}_2 \sigma_\mu \Psi_2, \\ \mu &= 0, 1, 2 \end{aligned} \quad (10)$$

In this approach one can define *meson* states [2,6]:

$$M_{ab,\alpha\beta} = \Psi_{b,\beta} \bar{\Psi}_{a\alpha}, \quad (11)$$

where Latin letters a, b denote color $SU(2)$ indices, and Greek letters α, β denote Lorentz spinor indices. One can re-express the meson state M , which is a 2×2 matrix in both color and Dirac space, in terms of the above bilinears [2];

$$\begin{aligned} M &= \mathcal{A}_3 \mathbf{1} \cdot \sigma_3 + \mathcal{A}_1 \mathbf{1} \cdot \sigma_1 + \mathcal{A}_2 \mathbf{1} \cdot \sigma_2 + \mathcal{A}_4 \mathbf{1} \cdot \mathbf{1} \\ &+ \mathcal{F}_{3,\mu} \gamma^\mu \sigma_3 + \mathcal{F}_{1,\mu} \gamma^\mu \cdot \sigma_1 + \mathcal{F}_{2,\mu} \gamma^\mu \sigma_2 + \mathcal{F}_{4,\mu} \gamma^\mu \mathbf{1}. \end{aligned} \quad (12)$$

The first matrix written is in Dirac space, and the second is in ‘‘ $SU(2)$ color’’ space.

The interesting feature of the $SU(2) \times U_5(1)$ model is that the parity-invariant condensate transforms as a $SU(2)$ triplet (9) and, hence, once formed, it breaks $SU(2) \rightarrow U(1)$ *dynamically* [2,6]. The parity-violating condensate, on the other hand, is an $SU(2)$ singlet. In continuum theories, the *energetically* preferable configuration in the *absence of external sources* is the parity-invariant condensate, according to the theorem of Vafa and Witten [25,1] on the impossibility of spontaneous parity breaking in *vectorlike* theories, which we shall discuss in the next subsection. Thus, at least from naive continuous considerations, one expects that *energetics* favors the formation of parity invariant condensates, and this was the main reason why parity violating condensates have been ignored, so far, in the existing literature. As we shall argue in the next subsection, this feature is respected by the *lattice* model of Ref. [6].

All these ideas can be incorporated into a rough phase diagram for a three-dimensional $SU(2) \times U(1)$ theory, proposed in Ref. [29]. The diagram is depicted in Fig. 1. The couplings shown are *inverse couplings*, $\beta_2 = 4/ag_2^2$, $\beta_1 = 1/ag_1^2$, where a is the lattice spacing.

The top line $\beta_2 = \infty$, $\beta_1 \neq 0$, corresponds to the QED₃ case. For QED₃ it is now generally accepted that there exists [1,5,30] a critical number of fermion flavors, below which there is dynamical formation of a chiral condensate and chiral symmetry breaking [1,3]. In the language of an effective theory, where the dimensionless coupling is taken to be the inverse of the number of fermion flavors [5], we can say that there is a *critical coupling* above which there is symmetry breaking.

In Fig. 1, the (inverse) critical coupling on the lattice is denoted as β_1^c . The shaded area shows the weakly coupled $SU(2)$ breaking, and the fact that we have no breaking on the $\beta_2 = 0$ (i.e., infinitely coupled) $SU(2)$ line, as discussed in Ref. [29] and will be reviewed below, means—by continuity—that one can draw a tentative critical line separating the broken and unbroken phases. The issue of whether the point where the line hits the $\beta_2 = 0$ axis is at the origin or at a finite value of β_2^c is one which we shall resolve here.

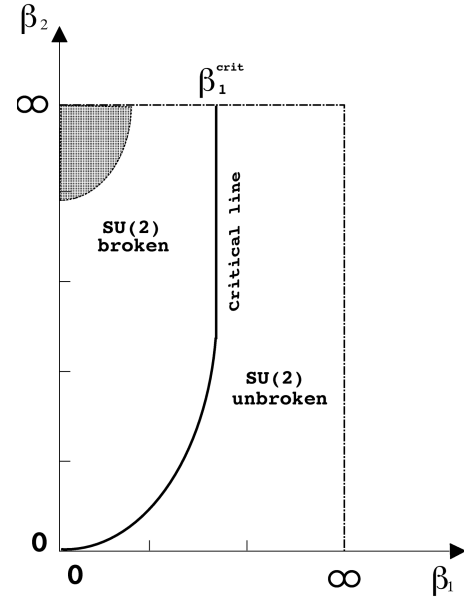


FIG. 1. Phase diagram for the $SU(2) \otimes U(1)$ model. The solid line is the critical line which is determined in this work, separating the phases of broken $SU(2)$ gauge symmetry from the phase where the symmetry is unbroken. Its precise shape is conjectural at present. Analytical and continuity arguments in this work determine the shape of the line in the neighborhood of $(\beta_1, \beta_2) = (0, 0)$ and $(\beta_1, \beta_2) = (\beta_1^c, \infty)$ only. This critical line also seems to characterize a solid state model, whose low-energy continuum limit is the gauge theory studied in this work.

We note at this point that, in the context of our statistical model [6], there is the special relation (5) among the (inverse) couplings of the $SU(2)$ and $U_5(1)$ factors, namely, $\beta_2 = 4\beta_1$, which, as we have mentioned, originates from the special structure of the magnon (CP^1) degrees of freedom of the model. This special relation is interesting in that, when combined with the fact that the gauge couplings in the statistical model depend on the doping concentration of the superconducting system, implies the existence of extreme values for the doping concentration, above or below which the broken- $SU(2)$ gapped phase is lost. As we shall argue in this work, the critical value $\beta_2^{\text{crit}} = 0$, which implies that in the context of the present effective theory one cannot see a minimum coupling below which the $SU(2)$ symmetry is restored. It is understood that in the condensed matter context such a minimum coupling, appropriate for the onset of antiferromagnetism, arises from the magnon CP^1 sector. We shall discuss such issues in more detail in Sec. VI.

B. Parity and fermions on the lattice

1. The Vafa-Witten theorem in the continuum

Before embarking into a detailed analytical study of the phase structure of $SU(2) \otimes U_5(1)$ theory, we would like first to devote some time on the important issue of parity symmetry for *lattice* gauge models. As is well known, in continuum models, an important theorem, due to Vafa and Witten [25], forbids the spontaneous breaking of parity symmetry in vectorlike theories, in the sense that the parity-violating conden-

sate is not energetically preferable. Let us briefly review this, in the context of our three-dimensional gauge model [6]. We shall consider the Euclidian path integral for the two different mass terms, corresponding to the condensates A_3 (parity preserving) and A_4 (parity violating). Let us start from the case where the $\langle \mathcal{A}_4 \rangle \neq 0$ condensate is formed. In this case, the relevant path integral reads

$$\begin{aligned} Z_{A_4} &= \int DAD\bar{\Psi}D\Psi \exp\left(\int d^3x[L[A] + \bar{\Psi}(i\mathcal{D} + im)\Psi]\right) \\ &= \int DA \det[i\mathcal{D} + im] \exp\left(\int d^4xL[A]\right) \end{aligned} \quad (13)$$

where $L[A]$ denotes the pure gauge part of the Lagrangian.

We can see that $\det[i\mathcal{D}]$ is positive because given $i\mathcal{D}\Psi = \lambda\Psi$ then $i\mathcal{D}(\gamma_2\sigma_2\Psi^*) = \lambda(\gamma_2\sigma_2\Psi^*)$. Thus every eigenvalue is repeated twice and the determinant (the product of the e values) is therefore real and positive. The gamma matrices are in Dirac space and the sigma matrices are in color space.

However, $\det[i\mathcal{D} + im]$ is *not real* for the following reason. The eigenvalue equations, in the presence of the mass m read

$$(i\mathcal{D} + im)\Psi = (\lambda + im)\Psi$$

and

$$(i\mathcal{D} + im)(\gamma_2\sigma_2\Psi^*) = (\lambda + im)(\gamma_2\sigma_2\Psi^*). \quad (14)$$

The two equations have the same eigenvalue, however, on squaring each eigenvalue we get a complex number and therefore the determinant is complex.

Let us now come to the case where the parity-invariant condensate is formed $\langle \mathcal{A}_3 \rangle \neq 0$. In this case, the effective action reads

$$Z_{A_3} = \int DA \det[i\mathcal{D} + im\sigma_3] \exp\int d^3xS[A]. \quad (15)$$

Applying the same method again we now get

$$(i\mathcal{D} + im\sigma_3)\Psi = (\lambda + im)\Psi,$$

and

$$(i\mathcal{D} + im\sigma_3)(\gamma_2\sigma_2\Psi^*) = (\lambda - im)(\gamma_2\sigma_2\Psi^*). \quad (16)$$

Now we see that the eigenvalues come in complex conjugate pairs, and therefore the determinant is real and positive.

Thus, the determinants in both cases have the same absolute value, but the determinant in the case of a parity-violating condensate has an extra phase factor making it complex. It is then straightforward to argue that the parity-violating case will not be energetically preferable [25]. To this end, we note that the vacuum energy (in a box of volume V) is given by

$$e^{-E_j V} = \int d\mu(A) e^{\int d^3xL[A]} \det_j, \quad (17)$$

where \det_j , $j=3,4$ denotes the result of the fermion determinant in the case where the A_3 or A_4 condensates are formed, respectively, and $d\mu(A)$ is the measure for the gauge field integration and is positive; the same is true for the exponential $e^{\int d^3xL[A]}$ in the Euclidean formalism. By a generic result in complex integration calculus, then, the phase in \det_4 can only make the integration smaller than that for \det_3 , and therefore the vacuum energy associated with mass $\langle \mathcal{A}_4 \rangle$ is larger than the vacuum energy for $\langle \mathcal{A}_3 \rangle$. So we can say that the *energetically preferred* mass term is the parity conserving one, and this is essentially the theorem of Vafa and Witten [25]. Caution should be expressed in applying the theorem to the case of dynamical mass generation, due to the absence of bare fermion masses, which leads to the existence of fermion zero modes, that make the Dirac operator ill defined, in need of regularization. However, the rigorous analysis of Ref. [25] deals with that case too.

2. Wilson fermions and the breakdown of the Vafa-Witten theorem on the lattice

On the lattice, however, the issue is nontrivial, and still unsettled. As argued recently [31], although the Vafa-Witten theorem [25] may hold in the continuum limit, however, on the lattice there may be terms (at least in an effective Lagrangian level), proportional to the lattice spacing a , which may violate explicitly the parity symmetry, thereby acting as external sources and hence spoiling basic assumptions of the Vafa-Witten theorem [25]. The issue of how the continuum limit is taken is therefore a tricky one, and currently there is a debate as to whether spontaneous breaking of parity occurs on the lattice [31,32]. Although we shall not enter this debate, which concerns Wilsonian fermions on the lattice that we do not use here, however, we consider it as useful to point out the difficulties associated with the parity symmetry, since it is a very important issue for the superconductivity mechanism of the models [4,6]. This will help the reader appreciate better how these problems are avoided in the specific lattice model of Ref. [6], which we use for our purposes in this work.

The main problem with the lattice formulations of the Vafa-Witten theorem, using Wilson fermions, is associated with the fact that, in the case of spontaneous breaking of parity, the Dirac operator has zero modes, as we shall discuss below, and thus needs regularization. Such a regularization is provided by adding appropriate sources (which may trigger parity breaking) in the effective action and then removing them. The presence of a source term violates the vectorlike nature of the regularized theory, and in general the problem arises from commuting the limits of removing the source or sending the bare mass term to zero.

Let us first review the situation in the case of four-dimensional gauge theories. The reduction to three-dimensional gauge theories with even number of fermionic species will be straightforward, as we shall argue below. In the case of lattice regularization with Wilson fermions, the appropriate Hermitean operator is not the Dirac operator but the overlap Hamiltonian $\gamma_5 W(m_0)$, where m_0 is a bare mass term needed for regularization of the Wilson-Dirac operator

W . This operator is known to have fermionic zero modes. The latter lead to a nonzero spectral density of eigenvalues $\rho(\lambda, m_0)$ around $\lambda=0$, in the limit of zero (bare) fermion mass. If $\tilde{\rho}$ denotes the density of the Dirac operator $-i\mathcal{D}$, then the following result holds [33]:

$$\rho(\lambda, m) = \frac{|\lambda|}{\sqrt{\lambda^2 - m^2}} \tilde{\rho}(\sqrt{\lambda^2 - m^2})$$

$$|\lambda| > m = 0 \quad |\lambda| \leq m. \quad (18)$$

As the fermion mass m tends to zero, the operator $\rho(\lambda, m) \rightarrow \tilde{\rho}(\lambda)$ *nonuniformly*.

To trigger numerically spontaneous breaking of a symmetry one adds an appropriate symmetry-breaking source term and then removes it. In the case at hand, one should add a source term of the form $ih\bar{\Psi}\gamma_5\sigma_3\Psi$. As noted in Ref. [32], then, the parity-violating condensate, proposed to occur in Wilson fermions [31], is proportional to $\rho(0, m_0)$ as the source term is removed, $h \rightarrow 0^\pm$:

$$\langle i\bar{\Psi}\gamma_5\sigma_3\Psi \rangle = \mp 2\pi\rho(0, m_0), \quad (19)$$

where m_0 is a bare mass term which should be removed, and for simplicity we assumed two fermion flavors.

The debate in the current literature [31,32] concerns the ordering of the limits $m_0 \rightarrow 0$, $h \rightarrow 0$ in the case of lattice theories with Wilson fermions. The presence of a nonzero physical mass m_0 renders the limit $h \rightarrow 0$ safe, the parity-violating condensate vanishes on *both* the lattice and the continuum formalisms, and, thus, there is no problem with the theorem of Ref. [25].

In three-dimensional lattice gauge theories, with an *even* number of fermionic species, as the models we are interested in, chiral and parity-symmetry breaking may be studied in full analogy with four-dimensional gauge theories, provided one works with a 4×4 reducible Dirac representation [1], generated by the following γ matrices:

$$\gamma^0 = \begin{pmatrix} \sigma_3 & \mathbf{0} \\ \mathbf{0} & -\sigma_3 \end{pmatrix}, \quad \gamma^1 = \begin{pmatrix} i\sigma_1 & \mathbf{0} \\ \mathbf{0} & -i\sigma_1 \end{pmatrix}, \quad \gamma^2 = \begin{pmatrix} i\sigma_2 & \mathbf{0} \\ \mathbf{0} & -i\sigma_2 \end{pmatrix}. \quad (20)$$

In such a case, there are two matrices that anticommute with the set of the γ -Dirac matrices [1]

$$\gamma_3 \equiv \begin{pmatrix} 0 & \mathbf{1} \\ \mathbf{1} & 0 \end{pmatrix}, \quad \gamma_5 \equiv i \begin{pmatrix} 0 & \mathbf{1} \\ -\mathbf{1} & 0 \end{pmatrix}. \quad (21)$$

Chiral symmetry is then generated by γ_5 , and is broken by the parity-invariant condensate, which in four-component notation for the spinors Ψ reads $A_3 = \langle \bar{\Psi}\Psi \rangle$. On the other hand, the parity-violating fermion condensate is given by $A_4 = \langle \bar{\Psi}\Delta\Psi \rangle$, with

$$\Delta \equiv i\gamma_3\gamma_5 = \begin{pmatrix} \mathbf{1} & 0 \\ 0 & -\mathbf{1} \end{pmatrix}. \quad (22)$$

It is, then, straightforward, following Ref. [32], to show that A_4 obeys a relation of the form (19) for the three-dimensional case.

We now remark that, in our condensed-matter inspired case (3), the fermions describing holon nodal excitations in the d -wave state are *Dirac spinors* (6) and *not Wilson*. According to the discussion in Ref. [34], for such a case there are no consistency problems or ambiguities, as far as results in the continuum are concerned [25]. To show this, in our case, one should first note that, as we shall discuss in more detail in the next section, the effective potential for the meson fields M (11) assumes the following generic form [2,29]:

$$V_{\text{eff}} \sim \text{Tr} \sum_i \left(A \ln M_i - \sum_\mu P[M_i(-\gamma_\mu)M_i^\dagger\gamma_\mu] \right), \quad (23)$$

where A is a numerical constant, $P(x)$ denotes an appropriate polynomial in x , i is the lattice site, and Tr is taken over the (reducible) 4×4 Dirac indices. As mentioned above to study spontaneous parity breaking numerically, one should add to Eq. (23) an appropriate source term:

$$V_S \equiv hM_i. \quad (24)$$

Following Ref. [34], we assume the following form for the vacuum wave function of M_i :

$$M_i = U e^{i\theta\Delta} = U(\cos\theta + i\Delta\sin\theta), \quad (25)$$

where Δ has been defined in Eq. (22).

From the specific M dependence of $P(x)$ in Eq. (23), one observes that the only dependence on θ comes through the source term

$$V_{\text{eff}}[h] \sim 4[hU\cos\theta + A\ln U - 3P(U^2)]. \quad (26)$$

By extremizing Eq. (26) with respect to θ , one obtains only the trivial minimum $\theta=0$, in contrast to the case of Wilson fermions, where the possibility for a nontrivial solution for θ exists, due to the Wilson parity-breaking term [34]. This solution implies that parity cannot be broken spontaneously, in agreement with the (continuum) theorem of Vafa and Witten [25].

Hence, for our purposes in this work from now on we assume that *dynamical mass generation* in our $SU(2) \times U_S(1)$ model selects—due to energetics—the parity-invariant combination, which is accompanied by the presence of Goldstone bosons due to the breaking of $SU(2) \rightarrow U(1)$ [2,6,29,35].

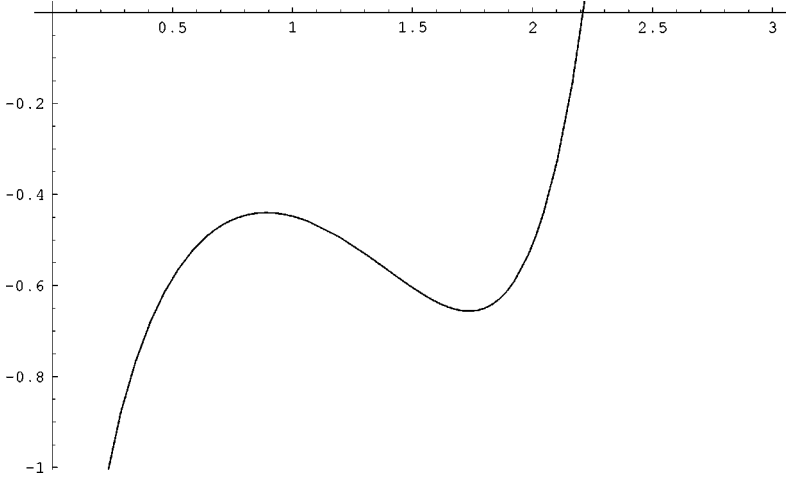


FIG. 2. The effective potential in the case $\beta_2 = \infty, \beta_1 = 0$, which coincides with the case of strongly coupled QED₃. The potential has stationary points, implying a nonvanishing chiral-symmetry breaking condensate.

III. STUDY OF THE PHASE DIAGRAM OF THE THREE-DIMENSIONAL $SU(2) \otimes U_S(1)$ LATTICE GAUGE THEORY

A. The phase diagram in the regime $\beta_2 = \infty, \beta_1$ arbitrary

In this regime of the phase diagram the system is equivalent to a strongly coupled QED₃, with global $SU(2)$ symmetry. This global symmetry acts like a flavor symmetry, and is represented by an index f . Because of this limiting procedure to QED₃, the spinors will be kept two component (6), so that a smooth transition to the case of nonzero $SU(2)$ coupling is guaranteed. The pertinent path integral is

$$Z = \prod_{i,\mu} \int dU_{i,\mu} d\bar{\Psi}_i^f d\Psi_i^f \exp(-S[\bar{\Psi}, \Psi, U]), \quad (27)$$

where S denotes the action (7), written as

$$\begin{aligned} S[\bar{\Psi}, \Psi, U] = & \frac{1}{2} K \sum_{i,\mu} \sum_f [\bar{\Psi}_i^f(-\gamma_\mu) \Psi_{i+\mu}^f U_{i,\mu} \\ & + \bar{\Psi}_{i+\mu}^f \gamma_\mu \Psi_i^f U_{i,\mu}^\dagger] + \beta_1 \sum_p (1 - \text{tr } U_p). \end{aligned} \quad (28)$$

Putting $\beta_1 = 0$, we can do the $U_S(1)$ integral immediately [2]:

$$\begin{aligned} \prod_{i,\mu} \prod_f \int dU_{i,\mu} \exp \left[-\frac{K}{2} \sum_{i,\mu} [\bar{\Psi}_i^f(-\gamma_\mu) \Psi_{i+\mu}^f U_{i,\mu} \right. \\ \left. + \bar{\Psi}_{i+\mu}^f \gamma_\mu \Psi_i^f U_{i,\mu}^\dagger] \right] = \prod_{i,\mu} \prod_f I_0^u(2\sqrt{y_{i,\mu}^f}) \end{aligned} \quad (29)$$

$$\begin{aligned} y_{i,\mu}^f & \equiv \frac{K^2}{4} \bar{\Psi}_i^f(-\gamma_\mu) \Psi_{i+\mu}^f \bar{\Psi}_{i+\mu}^f \gamma_\mu \Psi_i^f, \\ & = \frac{K^2}{4} \text{Tr}[M_i^f \gamma_\mu M_{i+\mu} \gamma_\mu]. \end{aligned} \quad (30)$$

The quantity $(M_i^f)^{\alpha\beta}$ denotes the meson field (making the Dirac indices explicit) $(\Psi_i^f)^\alpha (\bar{\Psi}_i^f)^\beta$. I_0^u denotes the zeroth order modified Bessel function [36], *truncated* to an order determined by the number of the Grassmann (fermionic) degrees of freedom in the problem [6,29]. In our case, because of the Dirac indices and 2 flavors of the *lattice spinors* Ψ , one should retain terms in I_0^u up to $\mathcal{O}(y^4)$:

$$I_0^u(2\sqrt{y_{i,\mu}^f}) = 1 + y_{i,\mu} + \frac{y_{i,\mu}^2}{4} + \frac{y_{i,\mu}^3}{36} + \frac{y_{i,\mu}^4}{576}. \quad (31)$$

The path integral is flavor symmetric $Z = \prod_f Z_f$ and, hence, we may factor out and ignore this dependence. We wish to obtain a path integral for the meson field M_i^f , which necessitates the inclusion of the Jacobian for the pertinent field transformation. This is calculated in Appendix B, following Ref. [26]. The result for the partition function reads

$$\begin{aligned} Z_f = \prod_{i,\mu} \int dM_i^f \exp \left[-\sum_i \log \det M_i^f + \sum_{i,\mu} \log I_0^u(2\sqrt{y_{i,\mu}^f}) \right] \\ = \prod_{i,\mu} \int dM_i^f \exp \left[\sum_{i,\mu} -\frac{1}{6} \log \det M_i^f M_{i+\mu}^f \right. \\ \left. + \log I_0^u(2\sqrt{y_{i,\mu}^f}) \right]. \end{aligned} \quad (32)$$

The effective potential depends on the variable y defined in Eq. (30). To determine its form, in terms of the condensate, one writes the vacuum expectation value (VEV) $\langle M_i^f \rangle = m^f W$ where W is a unitary matrix. So $\text{Det } M_i^f \sim m^2$ and $y_{i,\mu} \sim K^2 m^2 / 2$.

From the discussion in the previous section, we know that the energetically preferable configuration is the parity-conserving one, in which half of the fermion ‘‘flavors’’ acquire masses $+m$, and the rest acquire masses $-m$ [25,1]. Thus, the tree-level effective potential becomes, neglecting overall factors,

$$V_{\text{eff}} \sim \frac{2}{3} \log m - \frac{1}{2} K^2 m^2 + \frac{1}{16} K^4 m^4 - \frac{1}{72} K^6 m^6 + \frac{11}{3072} K^8 m^8, \quad (33)$$

which is plotted in Fig. 2 (with $K=1$).¹ This potential has stationary points and, from the arguments of [26] (described in Appendix B), this is sufficient to show that $\langle M_i^f \rangle \neq 0$.

The incorporation of the gauge interactions will change the situation, and induce nontrivial dynamics which may result in a change in symmetry for some regions of the gauge coupling constants. From the previous result (33), and the discussion in Sec. II, it becomes clear that for weak $SU(2)$ and strong enough $U_S(1)$ the $SU(2)$ symmetry is broken down to a $U(1)$ subgroup [2]. The nontrivial issue here is whether there exist critical (inverse) couplings β_i^c , $i=1,2$, above which the symmetry is restored. According to earlier analyses, either in the continuum or on the lattice [1,30,37], there appears to be a *critical coupling* β_1^c on the axis $\beta_2 = \infty, \beta_1 = \text{free}$, above which dynamical mass generation due to the $U_S(1)$ group cannot take place. This is depicted in Fig. 1.

In the large- N continuum theories [1] one usually identifies $8g_1^2 N = \alpha$, where α is kept fixed as $N \rightarrow \infty$, and plays the role of an effective ultraviolet cutoff. In our lattice action we may identify the inverse of our lattice spacing a^{-1} with $\alpha/8$, in which case $\beta_1^c \sim N_c$, with N_c the critical number of (four-component) fermion flavors, below which dynamical mass generation due to $U_S(1)$ occurs. To leading $1/N$ resummation [1], $N_c \sim 32/\pi^2$; incorporating $1/N^2$ corrections shifts this number slightly higher. The issue on the existence of a critical number is still not quite settled, and proper lattice simulations are needed in this respect. For our qualitative purposes, however, the large- N critical number will be sufficient.

B. Strongly coupled $SU(2) \otimes U_S(1)$ regime

In this section we commence our analysis of the effects of strongly coupled $SU(2)$ gauge interactions, by means of a small β_2 expansion.

¹The general case $K \neq 1$ amounts to adding an irrelevant K -dependent constant to the expression for the effective potential. This is an exclusive feature of the minimal gauge model (7), because in that case one may absorb K in the normalization of the fermion fields. However, in the presence of *additional* nonminimal fermion interactions, e.g., four-fermion interactions, which, as we shall see, may characterize realistic models of doped antiferromagnets in their superconducting phases, the constant K can no longer be absorbed in a normalization of the fermion fields, and hence its magnitude acquires physical significance. We shall address such issues in Sec. VI. For the purposes of this section, the minimal gauge model (7) will suffice.

1. The effective action for $\beta_2 = \beta_1 = 0$

First, we examine the model at the (limiting) point $\beta_2 = \beta_1 = 0$ (i.e., the origin of the diagram of Fig. 1). We absorb the parameter K in a redefinition of the fermion fields, because the action under consideration is only quadratic in Ψ fields.² In this case, one may integrate out first the $U_S(1)$ gauge field. The $SU(2)$ action, then, is separable into an integral on each link on the lattice [29]:

$$\int dV \left\{ 1 + \text{tr}(\bar{A}V)\text{tr}(AV^\dagger) + \frac{[\text{tr}(\bar{A}V)\text{tr}(AV^\dagger)]^2}{4} + \frac{[\text{tr}(\bar{A}V)\text{tr}(AV^\dagger)]^3}{36} + \frac{[\text{tr}(\bar{A}V)\text{tr}(AV^\dagger)]^4}{576} \right\}, \quad (34)$$

where the variable A are defined as follows:

$$A_{\mu}(x)_b^a = \bar{\Psi}_b(x+a) \gamma_\mu \Psi^a(x),$$

$$\bar{A}_{\mu}(x)_b^a = \bar{\Psi}_b(x) (-\gamma_\mu) \Psi^a(x+a). \quad (35)$$

The evaluation of these terms was first done by Samuel [27], whose formalism we follow here. The resulting partition function, now with all gauge fields integrated out, is

$$Z_0 = \prod_i \int d\bar{\Psi}_i d\Psi_i \prod_{i,\mu} \left\{ 1 + \frac{1}{2} \text{tr}(\bar{A}_{i,\mu} A_{i,\mu}) + \frac{1}{6} [\text{tr}(\bar{A}_{i,\mu} A_{i,\mu})]^2 - \frac{1}{12} \text{tr}[(\bar{A}_{i,\mu} A_{i,\mu})^2] + \frac{1}{48} [\text{tr}(\bar{A}_{i,\mu} A_{i,\mu})]^3 - \frac{1}{72} \text{tr}[(\bar{A}_{i,\mu} A_{i,\mu})^3] + \frac{17}{5760} [\text{tr}(\bar{A}_{i,\mu} A_{i,\mu})]^4 - \frac{1}{320} [\text{tr}(\bar{A}_{i,\mu} A_{i,\mu})]^2 \times \text{tr}[(\bar{A}_{i,\mu} A_{i,\mu})^2] + \frac{1}{1920} \text{tr}[(\bar{A}_{i,\mu} A_{i,\mu})^2]^2 \right\}. \quad (36)$$

Since we want Z_0 to be in the form $Z_0 = e^{S_{\text{eff}}}$ we exponentiate the above polynomial still keeping terms up to order $O(A\bar{A})^4$:

²This is because our lattice fermions are of Dirac type. In the Wilson fermion case, on the other hand, due to the Wilson and bare mass terms, that one is forced to add in the lattice action, the above normalization of the spinors by K cannot be done.

$$\begin{aligned}
Z_0 = & \prod_i \int d\bar{\Psi}_i d\Psi_i \exp \sum_{i,\mu} \left\{ \frac{1}{2} \text{tr}(\bar{A}_{i,\mu} A_{i,\mu}) \right. \\
& + \frac{1}{24} [\text{tr}(\bar{A}_{i,\mu} A_{i,\mu})]^2 - \frac{1}{12} \text{tr}[(\bar{A}_{i,\mu} A_{i,\mu})^2] \\
& - \frac{1}{48} [\text{tr}(\bar{A}_{i,\mu} A_{i,\mu})]^3 - \frac{1}{72} \text{tr}[(\bar{A}_{i,\mu} A_{i,\mu})^3] \\
& + \frac{1}{24} \text{tr}(\bar{A}_{i,\mu} A_{i,\mu}) \text{tr}[(\bar{A}_{i,\mu} A_{i,\mu})^2] + \frac{3}{640} [\text{tr}(\bar{A}_{i,\mu} A_{i,\mu})]^4 \\
& - \frac{29}{2880} [\text{tr}(\bar{A}_{i,\mu} A_{i,\mu})]^2 \text{tr}[(\bar{A}_{i,\mu} A_{i,\mu})^2] \\
& + \frac{1}{144} \text{tr}(\bar{A}_{i,\mu} A_{i,\mu}) [\text{tr}(\bar{A}_{i,\mu} A_{i,\mu})]^3 \\
& \left. - \frac{17}{5760} \text{tr}[(\bar{A}_{i,\mu} A_{i,\mu})^2]^2 \right\}. \quad (37)
\end{aligned}$$

We want to rearrange the $(\bar{\Psi}, \Psi)$ which make up the \bar{A}, A to get an effective action in terms of meson fields defined on site. The standard procedure for making an effective action in terms of meson fields is to rewrite each term in Eq. (36) as a function of $M^{aa,\alpha\beta} = \Psi^{a,\alpha} \bar{\Psi}^{a,\beta}$, e.g.,

$$\begin{aligned}
\text{tr}(\bar{A}_{i,\mu} A_{i,\mu}) &= \bar{\Psi}_i^{a,\alpha} (-\gamma_\mu)^{\alpha\beta} \Psi_{i+\mu}^{b,\beta} \bar{\Psi}_{i+\mu}^{b,\gamma} (\gamma_\mu)^{\gamma\delta} \Psi_i^{a,\delta}, \\
&= -\Psi_i^{a,\delta} \bar{\Psi}_i^{a,\alpha} \Psi_{i+\mu}^{b,\beta} \bar{\Psi}_{i+\mu}^{b,\gamma} (-\gamma_\mu)^{\alpha\beta} (\gamma_\mu)^{\gamma\delta}, \\
&= -\text{tr}_c M_i^{\delta\alpha} \text{tr}_c M_{i+\mu}^{\beta\gamma} (-\gamma_\mu)^{\alpha\beta} (\gamma_\mu)^{\gamma\delta}. \quad (38)
\end{aligned}$$

$\text{tr}_c M$ means we have traced over the color indices. However if we were to substitute in for M the expansion in terms of bilinears (12) we would find that the term containing \mathcal{A}_3 vanishes because of the traceless property of the Pauli matrix σ_3 . Thus the above rearrangement of $\text{tr}(\bar{A}A)$ will not be of any use if we want to get information on the VEV of \mathcal{A}_3 . We must thus look for an alternative rearrangement.

This alternative arrangement can be demonstrated if we look at the term $[\text{tr}(\bar{A}_{i,\mu} A_{i,\mu})]^2$, which is written out as

$$\begin{aligned}
[\text{tr}(\bar{A}_{i,\mu} A_{i,\mu})]^2 &= [\bar{\Psi}_i^{b,\alpha} (-\gamma_\mu)^{\alpha\beta} \Psi_{i+\mu}^{a,\beta} \bar{\Psi}_{i+\mu}^{a,\gamma} (\gamma_\mu)^{\gamma\delta} \Psi_i^{b,\delta}] \\
&\quad \times [\bar{\Psi}_i^{d,\epsilon} (-\gamma_\mu)^{\epsilon\zeta} \Psi_{i+\mu}^{c,\zeta} \bar{\Psi}_{i+\mu}^{c,\theta} (\gamma_\mu)^{\theta\eta} \Psi_i^{d,\eta}], \quad (39)
\end{aligned}$$

we can rearrange the $(\Psi, \bar{\Psi})$ which appear into *pairs* of meson states defined on each site.

$$\begin{aligned}
&\Psi_i^{b,\delta} \bar{\Psi}_i^{d,\epsilon} \Psi_i^{d,\eta} \bar{\Psi}_i^{b,\alpha} \Psi_{i+\mu}^{a,\beta} \bar{\Psi}_{i+\mu}^{c,\theta} \\
&\quad \times \Psi_{i+\mu}^{c,\zeta} \bar{\Psi}_{i+\mu}^{a,\gamma} \gamma_\mu^{\alpha\beta} \gamma_\mu^{\gamma\delta} \gamma_\mu^{\epsilon\zeta} \gamma_\mu^{\theta\eta}, \\
&= \text{tr}_c (M_i^{\delta\epsilon} M_i^{\eta\alpha}) \text{tr}_c (M_{i+\mu}^{\beta\theta} M_{i+\mu}^{\zeta\gamma}) \gamma_\mu^{\alpha\beta} \gamma_\mu^{\gamma\delta} \gamma_\mu^{\epsilon\zeta} \gamma_\mu^{\theta\eta}. \quad (40)
\end{aligned}$$

This time when we substitute in our bilinear expansion for $M_i^{ab\alpha\beta}$ we do not lose the part depending on \mathcal{A}_3 . We are no longer tracing over a single Pauli matrix, but rather over $\text{tr}(\sigma_3^2) = \text{tr}(1)$. This procedure will be justified if we find that there exists an energetically favorable nonzero VEV for \mathcal{A}_3 .

Also we see that the terms in the action which have an odd number of $(\Psi, \bar{\Psi})$ pairs [i.e., $O(A\bar{A})$ and $O(A\bar{A})^3$] vanish in this procedure since they cannot be arranged to solely produce *pairs* of mesons. There is a subtlety involved in calculating the $O(A\bar{A})^4$ term, which we describe in Appendix A.

Having followed this procedure for each term in the action the next step will be to substitute in for M , or more precisely for \mathcal{A}_3 , the VEV we are looking for. We also assume that the VEVs of all other bilinears are zero [2,35,29]. Therefore $\langle M_i^{ab,\alpha\beta} \rangle = U_i \sigma_3^{ab} \delta^{\alpha\beta}$. Following the above procedure for each term in the action (37) we have

$$\langle O(A\bar{A}) \rangle = 0,$$

$$\left\langle \frac{1}{24} [\text{tr}(\bar{A}_{i,\mu} A_{i,\mu})]^2 \right\rangle = \frac{4}{3} U_i^2 U_{i+\mu}^2,$$

$$\left\langle -\frac{1}{12} \text{tr}[(\bar{A}_{i,\mu} A_{i,\mu})^2] \right\rangle = \frac{4}{3} U_i^2 U_{i+\mu}^2,$$

$$\langle O(A\bar{A})^3 \rangle = 0,$$

$$\left\langle \frac{3}{640} [\text{tr}(\bar{A}_{i,\mu} A_{i,\mu})]^4 \right\rangle = \frac{3}{5} U_i^4 U_{i+\mu}^4,$$

$$\left\langle -\frac{29}{2880} [\text{tr}(\bar{A}_{i,\mu} A_{i,\mu})]^2 \text{tr}[(\bar{A}_{i,\mu} A_{i,\mu})^2] \right\rangle = \frac{116}{135} U_i^4 U_{i+\mu}^4,$$

$$\left\langle \frac{1}{144} \text{tr}(\bar{A}_{i,\mu} A_{i,\mu}) [\text{tr}(\bar{A}_{i,\mu} A_{i,\mu})]^3 \right\rangle = \frac{4}{9} U_i^4 U_{i+\mu}^4,$$

$$\left\langle -\frac{17}{5760} \text{tr}[(\bar{A}_{i,\mu} A_{i,\mu})^2]^2 \right\rangle = -\frac{17}{54} U_i^4 U_{i+\mu}^4. \quad (41)$$

One can now change path-integration variables, from fermion to meson fields \mathcal{M} . An important role in the dynamics of the system is played by the Jacobian of such a transformation, which is calculated in Appendix B following standard arguments [26]. Including the Jacobian we get

$$\begin{aligned}
Z_0 &= \prod_i \int d\mathcal{M}_i \exp \left\{ - \sum_{i,\mu} \left(-\frac{4}{3} U_i^2 U_{i+\mu}^2 \right. \right. \\
&\quad \left. \left. - \frac{143}{90} U_i^4 U_{i+\mu}^4 \right) - \sum_i 2 \log U_i^4 \right\}, \\
&= \prod_i \int d\mathcal{M}_i \exp \left\{ - \sum_{i,\mu} \left(-\frac{4}{3} U_i^2 U_{i+\mu}^2 \right. \right. \\
&\quad \left. \left. - \frac{143}{90} U_i^4 U_{i+\mu}^4 + \frac{2}{6} \log U_i^4 U_{i+\mu}^4 \right) \right\}, \quad (42)
\end{aligned}$$

which describes the dynamics in the $\beta_2 = \beta_1 = 0$ region of the phase diagram of Fig. 1. To get a simple saddle point effective potential we complexify the condensate U_i and write, following Ref. [26], $U_i U_{i+\mu} = U^2$. This is justified, since we assume that, in the general case, the condensate U_i should be the same for all odd sites and all even sites separately. In our path integral the radial part of the contour is irrelevant (see Appendix B) and we can choose $U_{\text{even}} = U e^{i\varphi}$ and $U_{\text{odd}} = U e^{-i\varphi}$. As we discuss in Appendix B, the minimum value of the effective potential occurs for $\varphi = 0$. The zeroth order effective potential is defined $V_{\text{eff}} = -S_{\text{eff}}/\text{vol}$:

$$V_{\text{eff}} = 8 \ln U - 4U^4 - \frac{143}{30} U^8, \quad (43)$$

which is plotted in Fig. 3.

We observe that it has a local maximum, but, as explained in Ref. [26], this still implies stability of the broken $SU(2)$ vacuum, due to the special properties of the Jacobian associated with the transformation from the $\Psi, \bar{\Psi}$ variables to the meson variables \mathcal{M} . This is reviewed briefly in Appendix B.

From Fig. 3 it is evident that there exists $SU(2)$ symmetry breaking even for the case of $\beta_2 = 0$. This implies that the critical line in the phase diagram of Fig. 1 passes through the origin. This is also the situation argued to characterize the statistical model of Ref. [6], which may describe high-temperature superconductivity.

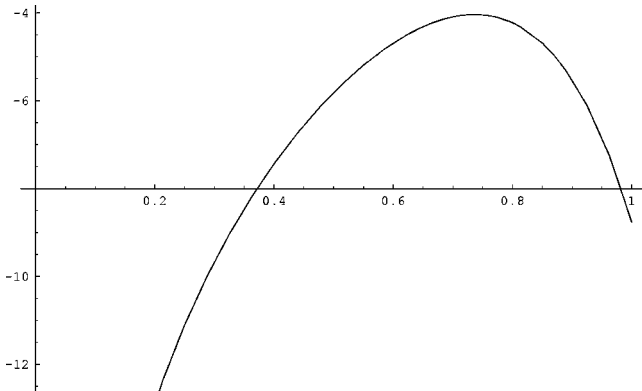


FIG. 3. The effective potential for $\beta_1 = \beta_2 = 0$.

2. Strong coupling expansion of β_2

We now look at the strong coupling expansion of the $SU(2)$ field, up to and including order $\mathcal{O}(\beta_2^2)$:

$$\begin{aligned}
\exp \left[-\beta_2 \sum_p (1 - \text{tr } V_p) \right] &\approx 1 - \beta_2 \sum_p (1 - \text{tr } V_p) \\
&\quad + \frac{\beta_2^2}{2} \sum_p (1 - \text{tr } V_p)^2 \\
&\quad \times \sum_q (1 - \text{tr } V_q) + \mathcal{O}(\beta_2^3). \quad (44)
\end{aligned}$$

The zeroth order term has been calculated in the previous section, Eq. (42).

The first order term in the $SU(2)$ integral is written

$$\begin{aligned}
Z_1 &= -\beta_2 \prod_{i,\mu} \int dV_{i,\mu} I_0^{\text{tr}}(2\sqrt{y_{i,\mu}}) \left(N_p - \sum_p \text{tr } V_p \right) \\
&= -\beta_2 N_p \prod_{i,\mu} \int dV_{i,\mu} I_0^{\text{tr}}(2\sqrt{y_{i,\mu}}) = -\beta_2 N_p Z_0 \quad (45)
\end{aligned}$$

because the addition of a single plaquette will give an odd number of group elements on each side of the plaquette, and therefore will integrate to zero.

At second order the calculation is no longer so simple,

$$\begin{aligned}
Z_2 &= \frac{\beta_2^2}{2} \prod_{i,\mu} \int dV_{i,\mu} I_0^{\text{tr}}(2\sqrt{y_{i,\mu}}) \\
&\quad \times \sum_p (1 - \text{tr } V_p) \sum_q (1 - \text{tr } V_q^\dagger), \quad (46)
\end{aligned}$$

by the same argument as used in the first order case, we can only have a nonzero integral where we avoid integrals over different numbers of V 's and V^\dagger 's. Thus the product $\sum_p (1 - \text{tr } V_p) \sum_q (1 - \text{tr } V_q)$ can be replaced by $(N_p^2 - \sum_p \text{tr } V_p^\dagger \text{tr } V_p)$,

$$\begin{aligned}
Z_2 &= \frac{\beta_2^2}{2} \prod_{i,\mu} \int dV_{i,\mu} I_0^{\text{tr}}(2\sqrt{y_{i,\mu}}) \left(N_p^2 + \sum_p \text{tr } V_p \text{tr } V_p^\dagger \right), \\
&= \frac{\beta_2^2 N_p^2}{2} Z_0 + \frac{\beta_2^2}{2} \prod_{i,\mu} \\
&\quad \times \int dV_{i,\mu} I_0^{\text{tr}}(2\sqrt{y_{i,\mu}}) \sum_p \text{tr } V_p \text{tr } V_p^\dagger. \quad (47)
\end{aligned}$$

Hence, the problem is to calculate the group integrals which make up the nontrivial part of Z_2 namely,

$$\begin{aligned}
 Z_2 &= \prod_{i,\mu} \int dV_{i,\mu} I_0^{\text{tr}}(2\sqrt{y_{i,\mu}}) \sum_p \text{tr} V_p \text{tr} V_p^\dagger \\
 &= \sum_p \prod_{i,\mu \in p} \int dV_{i,\mu} I_0^{\text{tr}}(2\sqrt{y_{i,\mu}}) \\
 &\quad \times \prod_{i,\mu \in p} \int dV_{i,\mu} I_0^{\text{tr}}(2\sqrt{y_{i,\mu}}) \text{tr} V_p \text{tr} V_p^\dagger \\
 &= \prod_{i,\mu} \int dV_{i,\mu} I_0^{\text{tr}}(2\sqrt{y_{i,\mu}}) \\
 &\quad \times \sum_p \frac{\prod_{i,\mu \in p} \int dV_{i,\mu} I_0^{\text{tr}}(2\sqrt{y_{i,\mu}}) \text{tr} V_p \text{tr} V_p^\dagger}{\prod_{i,\mu \in p} \int dV_{i,\mu} I_0^{\text{tr}}(2\sqrt{y_{i,\mu}})} \\
 &= Z_0 \sum_p J_p. \tag{48}
 \end{aligned}$$

The full path integral is then written as

$$Z = Z_0 \left(1 - \beta_2 N_p + \frac{\beta_2^2 N_p^2}{2} \right) + \frac{\beta_2^2}{2} Z_0 \sum_p J_p. \tag{49}$$

We will be interested in the logarithm of this function:

$$S_{\text{eff}} = \log \left[Z_0 \left(1 - \beta_2 N_p + \frac{\beta_2^2 N_p^2}{2} + \frac{\beta_2^2}{2} \sum_p J_p \right) \right], \tag{50}$$

which can be expanded, ignoring constant factors and keeping terms up to $O(\beta^2)$

$$S_{\text{eff}} = \log Z_0 + \frac{\beta_2^2}{2} \sum_p J_p. \tag{51}$$

Therefore, the strong coupling expansion leads us to calculate the group integrals around the plaquette in the function J_p

$$J_p = \frac{\prod_{i,\mu \in p} \int dV_{i,\mu} I_0^{\text{tr}}(2\sqrt{y_{i,\mu}}) \text{tr} V_p \text{tr} V_p^\dagger}{\prod_{i,\mu \in p} \int dV_{i,\mu} I_0^{\text{tr}}(2\sqrt{y_{i,\mu}})}. \tag{52}$$

The denominator has already been given earlier and is the product around each side of the plaquette of the $(A\bar{A})$ polynomial in Eq. (36). For convenience let us label the plaquette as having sides 1,2,3,4 and sites A, B, C, D

$$\begin{aligned}
 &\left\{ \prod_{i,\mu \in p} \int dV_{i,\mu} I_0^{\text{tr}}(2\sqrt{y_{i,\mu}}) \right\}^{-1} \\
 &= \left(1 + \frac{1}{2} \text{tr} A_1 \bar{A}_1 + \dots \right)^{-1} \left(1 + \frac{1}{2} \text{tr} A_2 \bar{A}_2 + \dots \right)^{-1} \\
 &\quad \times \left(1 + \frac{1}{2} \text{tr} A_3 \bar{A}_3 + \dots \right)^{-1} \left(1 + \frac{1}{2} \text{tr} A_4 \bar{A}_4 + \dots \right)^{-1}. \tag{53}
 \end{aligned}$$

These brackets can be expanded and truncated to $O(A\bar{A})^4$ since they still contain the Grassmann fields $(\Psi\bar{\Psi})$. The numerator contains a multitude of group integrals which need to be evaluated around the plaquette. The method, outlined briefly in Appendix C, is somewhat involved and the interested reader can refer to Ref. [38] for the algorithms used. It suffices to say that the terms which have an even number of $(\Psi\bar{\Psi})$ are kept since they will form the meson states.

After a tedious calculation along the above sketched lines, the quantity J_p becomes

$$\begin{aligned}
 J_p &= 1 + \frac{628}{81} (U_A U_B U_C U_D)^2 + \frac{1624}{135} (U_A U_B U_C U_D)^2 \\
 &\quad \times (U_A^2 U_B^2 + U_B^2 U_C^2 + U_C^2 U_D^2 + U_D^2 U_A^2) \\
 &\quad + \frac{548069}{18225} (U_A U_B U_C U_D)^4, \tag{54}
 \end{aligned}$$

and since in three dimensions we have one plaquette per link the effective potential to $O(\beta_2^2)$ is (again with $U_i U_{i+\mu} = U^2$)

$$\begin{aligned}
 V_{\text{eff}}(\beta_2^2) &= 8 \ln U - 4 U^4 - \frac{143}{30} U^8 - \frac{\beta_2^2}{2} \\
 &\quad \times \left\{ 3 + \frac{628}{27} U^8 + \frac{1624}{45} U^{12} + \frac{548069}{18225} U^{16} \right\}. \tag{55}
 \end{aligned}$$

This is plotted in Fig. 4, with β_2 taking a range of values between 0 and 0.5. The behavior does not change qualitatively as we increase β_2 , showing that the symmetry remains broken as we move up the β_2 of Fig. 1. This is as expected assuming a continuous critical line.

C. The phase diagram for $\beta_2=0$, $\beta_1 \neq 0$

Let us now complete our analysis on the phase diagram by concentrating on the region of strong $SU(2)$, $\beta_2=0$, keeping $U_S(1)$ coupling arbitrary (bottom horizontal axis of Fig. 1). In this part of the phase diagram one can *integrate out* the (strongly coupled) $SU(2)$ gauge fields to derive an effective action for the fermion and $U_S(1)$ gauge fields. The $SU(2)$ path integration is performed along the lines of Ref. [26]. In the strong coupling limit for $SU(2)$, $\beta_2=0$, the ef-

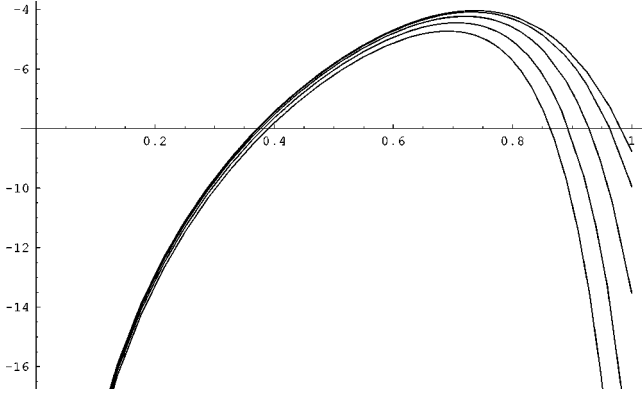


FIG. 4. The effective potential for $\beta_1=0$ and for $\beta_2 = 0, 0.125, 0.25, 0.375, 0.5$, the corresponding curves lying in order of decreasing magnitude of their maxima from right to left in the figure.

fective action, obtained after integration of the $SU(2)$ gauge fields, reduces to the sum of *one-link contributions* $S_{\text{eff}} = S_{\text{eff}}(A, \bar{A})$, with

$$\begin{aligned} A_{\mu}(x)_b^a &= \bar{\Psi}_b(x+a) \gamma_{\mu} U_{x,\mu}^{\dagger} \Psi^a(x), \\ \bar{A}_{\mu}(x)_b^a &= \bar{\Psi}_b(x) (-\gamma_{\mu}) U_{x,\mu} \Psi^a(x+a), \end{aligned} \quad (56)$$

where $U_{x,\mu}$ denotes the $U_S(1)$ group element, a is the lattice spacing, and the Latin indices a, b are color $SU(2)$ indices. Below we shall proceed to evaluate explicitly this strongly coupled effective action along the $\beta_2=0$ axis of the phase diagram in Fig. 1.

For the $SU(N)$ case the effective action $\exp(-S_{\text{eff}})$ is known in an expansion over A, \bar{A} [26]. This will be sufficient for our purposes here:

$$\begin{aligned} S_{\text{eff}} &= \frac{1}{N} \text{Tr}(\bar{A}A) + \frac{1}{2N(N^2-1)} \left[-\text{Tr}[(\bar{A}A)^2] \right. \\ &\quad \left. + \frac{1}{N} (\text{Tr}[\bar{A}A])^2 \right] + \dots + \frac{1}{N!} (\det A + \det \bar{A}) + \dots \end{aligned} \quad (57)$$

The determinant terms are associated with baryonic states [26]. We also note that for the $U(N)$ case the determinant terms are *absent*. In the phase diagram of Fig. 1 the $U(2)$ case occurs at the point $\beta_2 \rightarrow 0, \beta_1 \rightarrow 0$. We approach this point asymptotically, by working on the $\beta_2=0$ line, and assuming $\beta_1 \neq 0$. We first notice that the Abelian phase factors of the $U_S(1)$ interactions *cancel* from the expressions for the traces of A, \bar{A} in the effective action (57). Moreover, from the discussion of Sec. II, we know that the $SU(2)$ (strong-coupling) integration *cannot produce* a parity-invariant condensate, since the latter is not an $SU(2)$ singlet [2]. The resulting effective action should be expressible in terms of $SU(2)$ invariant fields. Thus, on the axis $\beta_2=0$ there is *no possibility* for the $U_S(1)$ group to generate a fermion con-

densate. This implies that for very strong $SU(2)$ group the symmetry is *restored* for arbitrary $U_S(1)$ couplings.

This is a very important fact, indicating the existence of a not well-defined limit $\beta_2, \beta_1 \rightarrow 0$, since from the discussion in this and the previous subsections it seems that there is an ordering problem in how one approaches the point $(\beta_1, \beta_2) = (0, 0)$. This indicates that the shape of the critical line around that point is the one depicted in Fig. 1, concaving upwards. By *continuity arguments*, then, one expects the shape of the entire critical line to be the one depicted in the figure. About the point $(\beta_1, \beta_2) = (\beta_1^c, 0)$, where the $SU(2)$ interactions are negligibly weak, and thus irrelevant, one expects an almost vertical shape of the critical line.

This discussion completes our analytical results for the phase diagram of the $SU(2) \otimes U_S(1)$ gauge theory. As we have already mentioned above, the derivation of the precise shape of the critical line, separating the phases of unbroken $SU(2)$ symmetry from the region where symmetry breaking occurs, requires a proper lattice simulation analysis, by means of a fermionic algorithm. We hope to be able to address these issues in a future publication. However, the above results will be sufficient for our purposes in this work, and will enable us to present physically interesting scenarios, pertinent to the physics of high-temperature superconductivity, which we shall discuss in Sec. VI.

Before doing so, it will be essential to review in the next two sections: (i) the symmetry breaking properties of our non-Abelian gauge model from the point of view of Goldstone's theorem and the existence of a local order parameter and (ii) the role of *nonperturbative effects*. These will be important in considering the coupling of the model to external electromagnetic fields, as required for the study of superconducting properties.

IV. KOSTERLITZ-THOULESS REALIZATION OF SUPERCONDUCTIVITY IN THE $SU(2) \otimes U_S(1)$ MODEL

This section is mainly a review of results that appear in the literature regarding the model [6,4,11]. It mainly serves as a comprehensive account, for the benefit of the nonexpert in the area, of the various delicate issues involved, which play a very crucial role in the underlying physics.

An important issue in the model (8) is the existence of a *global conserved symmetry*, namely, the fermion number, which is due to the electric charge of the fermions Ψ . The corresponding current is given by

$$J_{\mu} = \sum_{c=1}^2 \bar{\Psi}^c \gamma_{\mu} \Psi_c. \quad (58)$$

This current generates a global $U_E(1)$ symmetry, which after coupling with external electromagnetic fields is *gauged*.

In the absence of such external potentials, the symmetry $U_E(1)$ is *broken spontaneously* in the massive phase for the fermions Ψ . This can be readily seen by considering the following matrix element (see Fig. 5):



FIG. 5. Anomalous one-loop Feynman matrix element, leading to a Kosterlitz-Thouless-like breaking of the electromagnetic $U_{\text{em}}(1)$ symmetry, and thus superconductivity, once a fermion mass gap opens up. The wavy line represents the $SU(2)$ gauge boson B_μ^3 , which remains massless, while the blob denotes an insertion of the fermion-number current $J_\mu = \bar{\Psi} \gamma_\mu \Psi$. Continuous lines represent fermions.

$$S^a = \langle B_\mu^a | J_\nu | 0 \rangle, \quad a=1,2,3, \quad J_\mu = \bar{\Psi} \gamma_\mu \Psi. \quad (59)$$

As a result of the color group structure only the massless B_μ^3 gauge boson of the $SU(2)$ group, corresponding to the σ_3 generator in two-component notation, contributes to the graph. The result is [11,4]

$$S = \langle B_\mu^3 | J_\nu | 0 \rangle = (\text{sgn } M) \epsilon_{\mu\nu\rho} \frac{p_\rho}{\sqrt{p_0}}, \quad (60)$$

where M is the parity-conserving fermion mass (or the holon condensate in the context of the doped antiferromagnet). In our case this mass is generated *dynamically* by means of the $U_S(1)$ interactions, as we discussed above, provided the coupling constants were lying in the appropriate (strong) regime of the phase diagram of Fig. 1.

The result (60) is *exact* in perturbation theory, in the sense that the only modifications coming from higher loops would be a multiplicative factor $1/1 - \Pi(p)$ on the right hand side, with $\Pi(p)$ the B_μ^3 -gauge-boson vacuum polarization function [11].

As discussed in Refs. [4,11], the B_μ^3 color component plays the role of the *Goldstone boson* of the spontaneously broken fermion-number symmetry. If this symmetry is exact, then the gauge boson B_μ^3 remains *massless*. This is crucial for the superconducting properties [4], given that this leads to the appearance of a *massless pole* in the electric-current two-point correlators, the relevant graph being depicted in Fig. 6.

It can be shown [4] that in the massive-fermion [broken $SU(2)$] phase, the effective low-energy theory obtained after integrating out the massive fermionic degrees of freedom assumes the standard London action for superconductivity, the massless excitation ϕ being defined to be the *dual* of B_μ^3 :

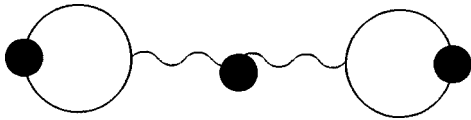


FIG. 6. The lowest-order contribution to the electric current-current correlator $\langle 0 | J_\mu(p) J_\nu(-p) | 0 \rangle$. The blob in the propagator for the gauge boson B_μ^3 indicates fermion loop (resummed) corrections. The blob in each fermion loop indicates an insertion of the current J_μ .

$$\partial_\mu \phi \equiv \epsilon_{\mu\nu\rho} \partial_\nu B_\rho^3. \quad (61)$$

All the standard properties of superconductivity, Meissner effect (strongly type II [4]), flux quantization, and infinite conductivity, follow then in a standard way, provided the excitation ϕ (and, hence, B_μ^3) is exactly massless.

Having discussed the spontaneous breaking of fermion number symmetry in the massive fermion phase, it is natural to inquire about the nature of symmetry breaking, in the sense of establishing the existence or absence of a local order parameter. In this respect, our discussion will parallel that of Ref. [4]. The neutral parity-invariant condensate $\langle \bar{\Psi}_1 \Psi_1 - \bar{\Psi}_2 \Psi_2 \rangle$, generated by the strong $U_S(1)$ interaction, is *invariant* under the $U(1) \otimes U_E(1)$, as a result of the τ_3 coupling of B_μ^3 in the action, and hence does not constitute an order parameter. This is a characteristic feature of our gauge interactions. Putative charge $2e$ or $-2e$ order parameters, such as the pairing interactions among opposite spins in the statistical model of [6,4],³ e.g., $\langle \Psi_1 \Psi_2 \rangle, \langle \bar{\Psi}_1 \bar{\Psi}_2 \rangle$ will vanish at any finite temperature, in the sense that strong phase fluctuations will destroy the vacuum expectation values of the respective operators, due to the Mermin-Wagner theorem. Even at zero temperatures, however, such VEVs yield zero result to any order in perturbation theory trivially, due to the fact that in the context of the effective B_μ^3 gauge theory of the broken $SU(2)$ phase, the gauge interactions preserve ‘‘flavor.’’ For a more detailed discussion on the symmetry breaking patterns of (2+1)-dimensional gauge theories, and the proper definition of order parameter fields, we refer the reader to the literature [11,4].

Thus, from the above analysis it becomes clear that gap formation, pairing and superconductivity can occur in the above model without implying any phase coherence.

V. INSTANTONS AND THE FATE OF SUPERCONDUCTIVITY

An important feature of our model is that, due to the non-Abelian symmetry breaking pattern $SU(2) \rightarrow U(1)$, the Abelian subgroup $U(1) \in SU(2)$, generated by the σ^3 Pauli generator of $SU(2)$, is *compact*, and may contain *instantons* [19], which in three space-time dimensions are similar to monopoles, and are known to be responsible for giving a *small but nonzero mass* to the gauge boson B_μ^3 ,

$$m_{B^3} \sim e^{-(1/2)S_0}, \quad (62)$$

where S_0 is the one-instanton action, in a dilute gas approximation. Its dependence on the coupling constant $g_2 \equiv g_{SU(2)}$ is well known [19]:

$$S_0 \sim \frac{\text{const}}{g_2^2}. \quad (63)$$

³In four-component notation, such fermionic bilinears correspond to $\langle \Psi \gamma_5 \Psi \rangle, \langle \bar{\Psi} \gamma_5 \bar{\Psi} \rangle$, considered in Ref. [4].

For weak coupling g_2 the induced gauge-boson mass can be very small. However, even such a small mass is sufficient to destroy superconductivity, since in that case there is no massless pole in the electric current-current correlator.

The presence of *massless* fermions, with zero modes around the instanton configuration, is known [19] to suppress the instanton effects on the mass of the photon, and under certain circumstances, to be specified below, the Abelian-gauge boson may remain exactly massless *even in the presence of nonperturbative effects*, thus leading to superconductivity, in the context of our model. This may happen [19] if there are extra global symmetries in the theory, whose currents connect the vacuum to the one-gauge-boson state, and thus they break spontaneously. This is precisely the case of the fermion number symmetry considered above. In such a case, the massless gauge boson is the Goldstone boson of the (nonperturbatively) spontaneously broken symmetry.

However, in our $SU(2) \otimes U_S(1)$ theory, discussed in this work, as a result of the (infinitely strong) $U_S(1)$ interaction, a mass for the fermions is generated, so we are not facing a problem with zero modes. Our analysis is based on a Wilsonian treatment, where massive degrees of freedom are integrated out in the path integral. This includes the gapful fermions, and the massive $SU(2)$ gauge bosons. The resulting theory, then, is a pure gauge theory $U(1) \in SU(2)$, and the instanton contributions to the mass of B_μ^3 are present, given by Eq. (62), in the one-instanton case.

We now remark that supersymmetry is known [19] to suppress instanton contributions. For instance, in certain $N = 1$ supersymmetric models with massless fermions, considered in Ref. [19] the instanton-induced mass of the Abelian gauge boson is given by

$$m_{\text{gauge boson}} \sim e^{-S_0} \quad (64)$$

which is suppressed, compared to the nonsupersymmetric case (62).

$N = 2$ supersymmetric theories in three space-time dimensions constitute additional examples of theories where the Abelian gauge boson remains exactly massless, in the presence of instantons [19,39]. Such theories have complex representation for fermions, and hence are characterized by extra global symmetries (such as fermion number). In view of our discussion above, such models will then lead to Kosterlitz-Thouless superconductivity upon gauging the fermion number symmetry.

We also remark that in supersymmetric theories of the type considered here and in Ref. [28], it is known [19] that supersymmetry cannot be broken, due to the fact that the Witten index $(-1)^F$, where F is the fermion number, is always nonzero. Thus, in supersymmetric theories the presence of instantons should give a small mass, if at all, in *both* the gauge boson and the associated gaugino. However, in three-dimensional supersymmetric gauge theories it is possible that supersymmetry is broken by having the system in a “false” vacuum, where the gauge boson remains massless, even in the presence of nonperturbative configurations, while the gaugino acquires a small mass, through nonperturbative effects. The life time, however, of this false vacuum is very

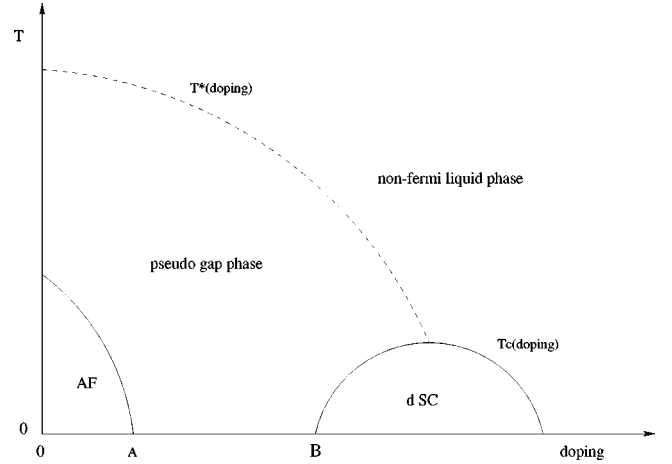


FIG. 7. The temperature-doping phase diagram summarizes the current (experimentally observed) situation in high-temperature superconducting cuprates. Notice the existence of an intermediate zero-temperature phase, characterized by the existence of pre-formed pairs, leading to a pseudogap.

long [19], and hence superconductivity can occur, in the sense that the system will remain in that false vacuum for a very long period of time, longer than any other time scale in the problem.

The short reviews of symmetry-breaking patterns and the role of nonperturbative effects, just presented, provided us with the necessary equipment to attempt a construction of possible scenarios, which might simulate the interesting physics underlying the high-temperature superconducting cuprates. A rather preliminary and Heuristic discussion will be presented in the next section. A more detailed analysis, especially in the context of the statistical models of Ref. [6], requires proper lattice simulations which automatically incorporate nonperturbative effects. This, however, falls beyond the scope of the present paper.

VI. APPLICATION TO THE PHYSICS OF HIGH-TEMPERATURE SUPERCONDUCTORS

A. Phenomenology of high-temperature superconducting materials

In this section we would like to consider a possible application of the above $SU(2) \otimes U_S(1)$ model [6] to the physics of high-temperature superconducting cuprates. Recent experiments [20] have demonstrated an extremely unconventional and rich structure of these materials, not in their superconducting phases, but rather in the normal phase. The phenomenology of the high-temperature cuprates may be summarized by the temperature-doping concentration phase diagram, shown in Fig. 7.

The phase diagram shows clearly a very low (including zero) doping antiferromagnetic phase (AF). Above a critical doping concentration (point A in Fig. 7), AF order is destroyed, but the interesting issue is the existence of a phase, named the “pseudogap phase,” which interpolates between the AF and the superconducting phases (dSC), the latter being known to be of d -wave type [13].

It is a general belief today, supported by many experimental results [20], e.g., results on optical conductivity, photoemission, transport, etc., that the pseudogap phase is characterized by pairing (“preformed pairs”), leading to the existence of a mass (pseudo) gap in the fermionic spectrum, which, however, is not accompanied by phase coherence. This situation is in sharp contradiction with standard BCS theories of superconductivity, according to which phase coherence appears simultaneously with the appearance of a gap.

The pseudogap phase is separated by a critical temperature curve $T_c(\text{doping})$ from the d -wave superconducting state, characterized by the sharp drop in resistivity, and strong type II superconductivity (penetration depth of external magnetic fields is of order of a few thousands of Å). Today, the general belief is that the superconducting pairing is of BCS type involving four-fermion interactions among the charged excitations. However, the four-fermion interactions do not have to be phononic.

The pseudogap phase is also separated by another curve $T^*(\text{doping})$ from the normal state phase, where there is no gap, but where there are abnormal normal state properties, such as linear dependence of the electrical resistivity with temperature for a wide range of temperature scales, etc. All such properties point towards a non-Fermi-liquid behavior of the normal state, which is experimentally observed, as far as we understand, not only in the regime of optimum doping, but well below it (shown in the Fig. 7).

B. Strongly coupled $U(2)$ gauge theory and the pseudogap phase

In this section we shall argue that the gauge theory $SU(2) \otimes U_S(1)$ of Ref. [6], whose low-energy limit has been studied in this paper in some detail, may provide a satisfactory qualitative explanation of the phase diagram of Fig. 7, especially as far as the appearance of a pseudogap phase is concerned. For the purposes of this article, we shall concentrate in the zero temperature region of the graph. Our method will be that of Ref. [40], i.e., approaching the pseudogap phase by studying the excitations about the nodes of the d -wave superconducting gap. We shall not deal here with excitations away from the nodes of the gap. Our hope will be that similar (long range) gauge-interaction phenomena are responsible for the formation of the bulk of the d -wave gap and the pseudogap. From the preliminary finite-temperature analysis of Ref. [40] it becomes clear that the gaps that open up at the nodes disappear at much lower temperatures ($T < 0.1$ K) than the bulk of the d -wave type gap [$T_c = \mathcal{O}(100$ K)], and this means that the predictions made in this work, if true, can be realized only if one looks at low temperatures.⁴

⁴However, we point out that the presence of external magnetic fields may enhance these values [40], as, for instance, is the case of the experiments involving thermal conductivity measurements [41]. See discussion at the end of this section.

Before starting our analysis on the (zero-temperature) pseudogap phase, we should point out that the gauge theory at hand, is also in agreement with deviation from Fermi-liquid behavior in the normal (no mass gap) phase. Indeed, as we discussed in previous articles [42], a $U(1)$ fermion-gauge theory in $2+1$ dimensions, in which the mass of the fermions is generated only dynamically through the gauge interactions, is characterized by nontrivial infrared fixed points, which according to general arguments [43] is sufficient to drive the theory away from the Landau-Fermi liquid (trivial infrared structure).

Let us continue our discussion on the diagram of Fig. 7 by considering the antiferromagnetic phase. In such a phase, the only excitations are assumed to be spin degrees of freedom. There are no charged excitations, and the pertinent dynamics is described by the magnon z sector of the model (3). As the doping exceeds a critical concentration (point A in Fig. 7), the antiferromagnetic order is destroyed. In the context of simple low-energy CP^1 models, which describe adequately the dynamics of the AF sector, this can be seen easily by applying renormalization-group arguments [44,45], and taking into account the dependence of the respective coupling constant on doping, in the way explained in Refs. [4,15].

The important question is whether superconductivity does not set in immediately, but one has to pass through the intermediate phase AB , where a “pseudogap” appears, but no phase coherence exists. As we shall argue now, our strongly coupled gauge theory $SU(2) \otimes U_S(1)$, presented above, may offer an explanation for the phenomenon.

To this end, we first remark that above the critical doping concentration that marks the on-set of disorder (A in Fig. 7), the z magnons are massive, with masses which themselves depend on the doping concentration [45,15,22]. In this regime, there are both charge and spin (z field) excitations. Integrating out the massive magnons z , the long-wavelength dynamics of the charge excitations is described by the effective $SU(2) \otimes U_S(1)$ gauge theory of Ref. [6], (8). The gauge $U_S(1)$ interaction is capable of inducing dynamical opening of a holon gap (pairing) if the pertinent coupling constant of the statistical model lies inside the $SU(2)$ broken regime of the phase diagram of Fig. 1.

We now remark that in the statistical model (3), which will be the basis of our discussion in this section, the inverse couplings of the $SU(2)$ and $U_S(1)$ gauge groups lie in the straight line AB depicted in Fig. 8, as a result of Eq. (5). In the condensed-matter model of Ref. [6], then, the local gauge group is $U(2)$ rather than $SU(2) \otimes U_S(1)$.⁵

At present, the precise shape of the critical line is not known, since it requires the construction of an appropriate fermionic algorithm, which will allow for a proper lattice study of the model. The strong coupling analysis in this paper has demonstrated, however, that the critical line passes through the origin of the graph, concaving upwards in the

⁵This, however, does not affect the results of the previous analysis pertaining to the mass generation. The only difference of the $U(2)$ case is the *absence* of *baryons* from the spectrum [26].

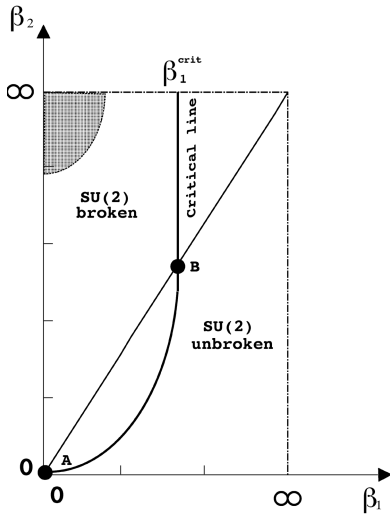


FIG. 8. Phase diagram for the $SU(2) \times U_S(1)$ gauge theory, viewed as a low-energy continuum limit of the solid-state model for doped antiferromagnets of Ref. [6]. The straight line indicates the specific relation of the coupling constants in the model.

way shown in the figure. Also, from the behavior of the critical line about the point $(\beta_2 = \infty, \beta_1^c)$, it is evident from the graph of Fig. 8 that the intersection point B defines an upper bound for the inverse coupling β_1 , in order for the system to be in the mass-generation phase. For all practical purposes it is qualitatively meaningful to assume an almost vertical shape of the critical line at the intersection point B , which implies that the critical coupling for mass generation for the coupling β_1 in the statistical model is still given by the single $U(1)$ gauge theory critical coupling, i.e., $\beta_1 < \beta_1^c$ (see Fig. 1). It is known that $\beta_1^c \sim 32/\pi^2$ [1,37]. So, on account of our discussion in Sec. III A and Eq. (5), such a gauge pairing would occur in the following range of doping concentrations:

$$\delta_{AF} < \delta < \delta_c^{(2)} \equiv 1 - \frac{\pi^2 \Lambda}{32 J}, \quad (65)$$

where δ_{AF} denotes the doping concentration at which the AF order is destroyed and Λ is the ultraviolet cutoff, which, in our lattice model, may be identified with the inverse of the lattice spacing a , as discussed at the end of Sec. III A.

This phase is characterized by the breaking of chiral symmetry. However, as discussed in Refs. [11,4], and reviewed in Sec. IV, the symmetry breaking occurs *without* a local order parameter. Strong phase fluctuations destroy the putative order parameter for $(2+1)$ -dimensional QED. This is an *exclusive feature* of the $2+1$ gauge interactions, and as we argue now, it is responsible for the appearance of a pseudogap. The concept of the pseudogap is associated precisely with the presence of a nonvanishing mass gap and thus the existence of “preformed pairs” in underdoped cuprates [20], but in absence of a local order parameter (phase coherence) in the model. The situation is analogous to the Kosterlitz-Thouless mode of symmetry breaking [12]. The important issue to understand is why there is no superconductivity in the model.

This issue is related to the presence of instantons, discussed in the previous section, which are responsible for giving a small but finite mass to the gauge boson B_μ^3 , and thus destroying the basic criterion of superconductivity (see Fig. 6). The presence of fermions does not change this. In the broken $SU(2)$ (gapped) phase of the model (8) the fermions are already massive, due to the extra $U_S(1)$ interactions, and hence there is no issue of zero modes that could screen the instanton effects. From Eq. (62), as well as the fact that the one-instanton action exhibits the following dependence on the $g_{SU(2)}$ coupling constant for the case at hand [19]:

$$S_0 \sim \frac{\text{const}}{g_{SU(2)}^2}, \quad g_{SU(2)}^2 \propto J(1-\delta) \quad (66)$$

one observes that the instanton-induced B_μ^3 -boson mass decreases upon increasing the doping concentration δ in the sample.

In the context of the statistical models of Ref. [6], etc., one should also consider the coupling of superconducting planes, by means of Coulomb interactions among the charge carriers (electrons). Such interactions may result in a small leakage of electrons across the planes, which inevitably leads to fermion-number nonconservation on the plane. In Ref. [28], within a spin-charge separating framework, such an interplanar coupling has been represented by inserting in the path-integral a term of the form

$$\int d\eta e^{2i \int d^3x \bar{\eta} \Psi^\alpha z_\alpha + \text{H.c.}}, \quad (67)$$

where $\alpha=1,2$ runs over “colors” in the model of $SU(2)$, and η is a Majorana spinor. Due to this, the term (67) in the effective action violates fermion number, and is interpreted as implying a hopping of *both* spin (z) and charge (Ψ) degrees of freedom. Notably, η may play the role of the supersymmetric partner of the B_μ^3 gauge boson, in a $N=1$ supersymmetric formulation of the model,⁶ which is possible upon certain relation [28] among the couplings of the microscopic spin-charge separating model of Ref. [6].

The explicit breaking of the fermion number symmetry by the interplanar coupling, as well as the absence of fermion zero modes in the massive phase [due to the $U_S(1)$ interactions] imply that the presence of fermions will not cancel the instanton-induced small mass of the gauge boson (62).⁷ In such a case, then, the gapped phase will be characterized by the presence of pairing, mass gap, but no phase coherence

⁶This supersymmetry carries nontrivial dynamical information about the spin-charge separation mechanism underlying the model, and hence it is different from the nondynamical global supersymmetry algebras, at specific points of the coupling constants, discovered in Ref. [46].

⁷Although, a reduction of order (64) might be expected in $N=1$ supersymmetric cases [28], occurring for particular values of doping. See discussion below.

and superconductivity, features shared by the pseudogap phase observed in cuprates (Fig. 7).

The above considerations are rather Heuristic at present. The complete analysis would necessitate a lattice simulation of the model (7) in the presence of instanton effects [in the broken phase after mass generation due to $U_S(1)$ interactions]. Analytical results at present exist only for $N=2$ supersymmetric theories, as we mentioned above [19,39], which, however, seem not to correspond to the physics of the cuprates [28], which appear to have at most $N=1$ supersymmetry upon coupling of the superconducting planes. Supersymmetry suppresses instanton effects in some cases (64), and some times may lead to a massless gauge boson, although such a case at present seems to characterize $N=2$ supersymmetric theories. We hope to return to a more detailed study of such issues in the future.

The suppression of instanton effects by supersymmetry, which in our class of statistical models may occur for certain doping concentrations [28] points to the following possibility: As one increases the doping concentration, a region is reached where there is a special relation among the various coupling constant of the effective spin-charge separating theory, leading to a $N=1$ supersymmetry [28]. For instance, in the context of models of Ref. [15] such a supersymmetric point could be reached for doping concentrations δ^* , such that $t' \sim \sqrt{JJ'}(1-\delta)^{3/2}$, where the prime denotes next-to-nearest-neighbor hopping (t) and Heisenberg exchange energies (J). By tuning the couplings one may arrange—always in the context of phenomenological models—for a situation in which $\delta^* \leq \delta_c^{(2)}$. This would imply that, within the region of dopings for which the gauge statistical interactions are responsible for the opening of a gap and pairing, the suppression of instanton effects due to the presence of (supersymmetric) fermions may be sufficient to allow for a gauge-theory-induced Kosterlitz-Thouless (KT) superconducting gap at the d -wave nodes. The KT nature of the gap implies that once opened such a gap cannot affect the d -wave character. This scenario for superconductivity has been advocated in Ref. [6]. In a related, but less probable, scenario, the tunneling to a ‘false’ supersymmetry-broken vacuum [19] could occur in the dSC region of the phase diagram (see Fig. 7).

C. Superconducting phase and additional four-fermion interactions

Despite these appealing scenaria for the role of gauge (spin-spin) interactions for inducing KT superconducting gaps at the nodes, in the realistic situation the onset of (d -wave) superconductivity occurs at higher doping concentrations, for which the attractive four-fermion couplings among charged excitations in the effective field theory become strong enough, so as to overcome the gauge interactions, and lead to a standard BCS type pairing among the charged excitations.

In such a case one then is forced to consider the effect of additional contact interactions, among the *holons*, which are up and above the gauge interactions considered so far. The simplest, and most likely the most relevant, of such interac-

tions are contact *four-fermion* interactions [47,4]. From a microscopic point of view such interactions may arise as an effective way to describe the tendency of holes to occupy nearest-neighbor lattice sites [4,18], or in some recent scenaria they may describe attractions due to screened Coulombic interactions among charged excitations, as a result of the interplanar coupling [48]. The corresponding coupling constant will again depend on the doping concentration [4], and this will imply interesting phase structures.

The additional four-fermion interactions are, then, viewed as being responsible for the appearance of an ordered d -wave state, with the gap being characterized by four nodes. We shall be fairly phenomenological, given that a detailed incorporation of extra four-fermion interactions in our strongly coupled gauge model is not straightforward. However, a phenomenological analysis will be sufficient to demonstrate the main unconventional features of our scenario for high-temperature superconductivity, at least in the context of a continuum effective field theory.

It is known that, in the context of relativistic models we consider here, as a result of linearization about the nodes of a d -wave superconducting gap, the four-fermion interactions are the only ones which become renormalizable (relevant) in the $1/N$ framework, where N is a flavor number for fermions. As an instructive example, consider, for instance, Gross-Neveu-type four-fermion couplings in the effective Lagrangian [21]

$$L_{4f} = \kappa \sum_{a=1}^2 (\bar{\Psi}_a \Psi^a)^2, \quad (68)$$

where Ψ_a are the relativistic spinors (6) describing the excitations about the nodes of a d -wave gap.

From standard arguments [49] on the phase structure of Gross-Neveu type couplings, we are considering here, we know that pair formation, and hence mass generation, in four-fermion theories occurs for dimensionless inverse couplings $\lambda \equiv 1/2\kappa\Lambda$ weaker than a critical value $2/\pi^2$. However, the full phase diagram, incorporating the $SU(2)$ and $U_S(1)$ couplings as well, as appropriate for the model of Ref. [6], will be more complicated. However, for our purposes in the present work it will be sufficient to consider only the effects of the $U_S(1)$ coupling, responsible for the mass generation in the model.

A phase diagram for an Abelian gauge theory with extra four-fermion interactions (of Gross-Neveu type) has been derived analytically in the context of a Schwinger-Dyson large fermion-flavor analysis in Ref. [4], and in principle the result can be checked in lattice models. For our purposes in this work it will be sufficient to assume the validity of the large-flavor-number continuous results of Ref. [4], and concentrate on the pertinent phase diagram in the coupling constant space between the gauge g and four-fermion couplings κ , depicted in Fig. 9.

In toy models of doped antiferromagnets [18,15], which are sufficient for our illustrative purposes, such Gross-Neveu four fermion terms are expressing the tendency of holes to break as less bonds as possible in the antiferromagnetic lattice, which is the configuration featuring the holes sitting

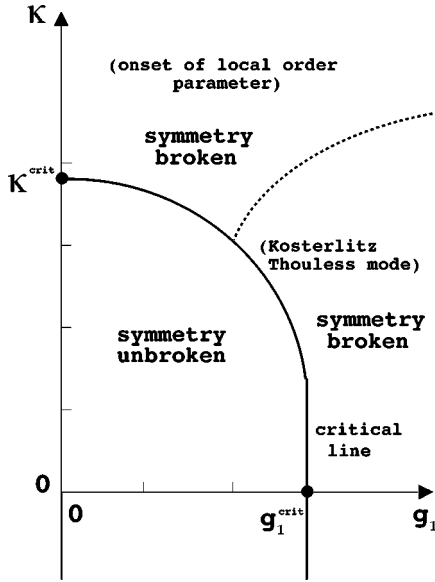


FIG. 9. A generic phase diagram of the theory with $U_S(1)$ gauge and four-fermion (Gross-Neveu) interactions. The critical line separates the phase of unbroken symmetry from that of broken symmetry. The symmetry breaking is due to the fermion condensate. The dotted line is conjectural at present, and indicates the on-set of a local order parameter due to the dominance of four-fermion interactions.

next to each other. Such interactions, may be described by adding to the Hamiltonian *attractive* four-fermion interactions of the form

$$-\kappa: \psi_1^\dagger \psi_1(j) :: \psi_2^\dagger \psi_2(j+1):, \quad (69)$$

where $\psi_\alpha, \alpha=1,2$ are Grassmann (holon) operators, j denote lattice site, and $: \dots :$ denotes normal ordering of quantum operators. The normal ordering conventions are such that a fermion bilinear is written as

$$\psi^\dagger \psi = : \psi^\dagger \psi : + \langle \psi^\dagger \psi \rangle, \quad \langle \psi^\dagger \psi \rangle = \delta \quad (70)$$

with δ the doping concentration in the sample. Such terms may be assembled, in the continuum, low-energy, limit [15,4], into Gross-Neveu four-fermion terms of the form (68), where the spinors are constructed as in Eq. (6).

At this stage, the coupling constant κ is a phenomenological parameter. However, from quite generic arguments, one would expect it to increase upon increasing the doping concentration δ in the sample, since the larger the doping, the bigger the probability of the holes to lie in adjacent sites of the lattice.

At present, the only case where four-holon-operators appear with well-defined coupling constants in terms of the microscopic parameters of the theory, is the t - j or Hubbard model case, where, however, the four-fermion interactions are *repulsive* [15,47]. In the models of Ref. [15], for instance, such Hubbard four-fermion couplings κ_{Hubbard} assume the generic form

$$\kappa_{\text{Hubbard}} \propto \kappa_0(t', J') \frac{1}{1-\delta}, \quad (71)$$

where $\kappa_0(t', J')$ is an appropriate function of the next-to-nearest-neighbor hopping element and Heisenberg exchange energies.

Combining Eq. (69) with such repulsive interactions, one then arrives at a generic coupling for four-holon (Gross-Neveu) operators in the model of the form

$$\kappa_{4f} = \kappa(\delta) - \kappa_0(t', J') \frac{1}{1-\delta}, \quad (72)$$

where $\kappa(\delta)$ is, at present, a phenomenological parameter, which, however, is expected to increase, as we said, with increasing δ . For the four-fermion interactions to be attractive one needs $\kappa_{4f} > 0$, and this places restrictions on the regime of doping, for which the interactions are going to lead to dynamical mass gap generation. When combined with the phase diagram of Fig. 9, this implies that pairing due to four-fermion interactions would occur for doping concentrations in a region determined by the critical line of Fig. 9. By appropriately choosing κ_{4f} , in the context of phenomenological models, it is then possible to arrange for a situation like the one depicted in Fig. 7, where the zero-temperature pseudogap phase interpolates between the AF and the standard BCS-type d -wave superconducting theory.

Notice that the dynamical mass generation due to four-fermi couplings leads to a *second order* transition, at zero temperatures, and hence to phase coherence, as is standard in BCS-type pairing. This should be contrasted with the gauge situation described above, which leads to Kosterlitz-Thouless-type breaking [11,4,6]. It would probably imply the existence of a crossover line (dotted) in the diagram of Fig. 9, separating the region of the broken symmetry phase where a local order parameter is present, due to the dominance of the four-fermion interactions, from the region where the Kosterlitz-Thouless mode of symmetry breaking (absence of a local order parameter) occurs, due to the dominance of the gauge interactions. Such phase diagrams should be confirmed by detailed lattice simulations, using appropriate fermionic algorithms, which fall beyond the scope of the present work.

The interesting feature is that *experimentally* one can make a distinction between a gap induced by the gauge interactions, or by four-fermion interactions, as a result of different scaling of the mass gap with an externally applied magnetic field. A suggestive experiment along these lines is that of Ref. [41], measuring the behavior of the thermal conductivity, in both the superconducting and ‘‘pseudogap’’ phases. Details on such issues are discussed in Refs. [40,50,51,21].

VII. CONCLUSIONS

In this work we have described a strong coupling expansion for an $SU(2) \otimes U_S(1)$ gauge theory, in three-dimensional space time. From the physical point of view, such models may serve either as a prototype for physical

applications to the physics of excitations about nodes in a d -wave high-temperature superconductor [6] or—when formulated in Euclidean lattices—as describing high-temperature phases of four-dimensional gauge theories of the early universe.

Our analysis has indicated a phase diagram of the form depicted in Fig. 1. The analytical results obtained in the present article pertained to the strongly coupled $SU(2)$ sector. We have shown the absence of a finite critical coupling for $SU(2)$ symmetry breaking. The breaking of $SU(2)$ is induced by dynamical parity-conserving mass generation due to the $U_S(1)$ strongly coupled sector. The shape of the critical line, separating the phases of broken $SU(2)$ symmetry, is still conjectural, since it requires proper lattice simulations with dynamical fermions, which is under consideration at present.

An important ingredient in our analysis, which was motivated from our condensed-matter ancestor models [6], was the use of “naive” Dirac spinors on the lattice, and *not* Wilson fermions. The latter are known to violate explicitly parity-symmetry breaking, due to the Wilson term. This may lead to spontaneous violation of parity symmetry [34,31], and therefore to a completely different phase diagram, although the issue is still unsettled [32].⁸

An interesting application of our strongly coupled gauge theory $SU(2) \otimes U_S(1)$ was argued to be provided by a possible explanation of the (zero-temperature) pseudogap phase between the antiferromagnetic and d -wave superconducting phases of the high-temperature cuprates (see Fig. 7). Due to the special symmetry breaking patterns, $SU(2) \rightarrow U(1)$ in the phase where a fermion mass is generated dynamically by the $U_S(1)$ statistical interactions in the model [6], and the existence of instanton configurations in the compact $U(1) \in SU(2)$, a small mass for the $U(1)$ gauge boson can be generated. Such a small mass, although does not prevent pairing, however, it spoils superconductivity, since it leads to the disappearance of the massless pole in the electric current two-point correlators. As explained in the text, in such a sector, the gauge theory is responsible only for the opening

of a mass gap in the fermion spectrum. However, the mode of symmetry breaking is of Kosterlitz-Thouless type, and hence no order parameter exists, since strong phase fluctuations destroy it (the parity-invariant fermion mass gap in the model of Ref. [6] is not an order parameter, since it is invariant under the respective symmetries, and hence there is no contradiction with the Mermin-Wagner theorem). Such a KT mass gap may be viewed as a pseudogap. In our scenario above, such a gap owes its presence to relativistic fermions at specific points of the fermi surface (e.g., nodes of the d -wave gap), argued to play a crucial role in the pertinent phase. We stress once more, that the important point in our approach [6] was the Kosterlitz-Thouless nature of the gauge symmetry breaking induced by gauge interactions in $2+1$ dimensions [11,4], which discriminates our approach from others [22,23].

Our belief that spin-gauge interactions may play a crucial role in the underdoped and normal phase of the high- T_c cuprates is strengthened by the abnormal properties of these phases [20], including the explicit observation of phase separation in the so-called stripe phase, occurring for a particular doping concentration [53]. In the d -wave superconducting phase, four-fermion BCS-like pairing may indeed occur, although the attractive four-fermion interactions, most probably, are not due to phonons, but of electronic origin [48].

In the presence of *both* types of interactions, gauge and four-fermion, the effective theory model presents interesting phases. One way to determine the origin of the dynamically induced mass gap in the various phases is to study the behavior of the system under the influence of external fields, as in the experiment of Ref. [41]. It is known [50,40,21] that the gauge-field induced mass gap scales differently with an applied magnetic field as compared to the gap induced by four-fermion Gross-Neveu-type interactions. Such a scaling may be determined by studying the thermal conductivity in the presence of an externally applied magnetic field, as in the experiments of Ref. [41]. Details of this analysis appear in Ref. [21].

We are, of course, aware that the simple, effective gauge field theory analysis we have just presented, may not be sufficient to explain quantitatively the rich phenomenology of the high-temperature cuprates. We believe, however, that it constitutes a step in this direction. Our hope is that, due to the simplicity and universality that underlies the superconducting models based on the gauge symmetry approach, our results capture essential features of the physical mechanism(s) underlying various phases of high-temperature superconductors, in much the same way as the single phonon BCS theory describes adequately the complicated physics of phononic superconductors. Moreover, as particle theorists, we also find this exercise very interesting, since it may imply that certain phenomena, characterizing the physics of the early universe, may have interesting counterparts in condensed-matter physics, and in particular the high-temperature (antiferromagnetic) superconductors. In this respect, specific mention should be made again to the work of Volovik [24], who pursues the analogies between particle and condensed matter physics, by suggesting solid-state experiments, involving superfluid helium, as possible labora-

⁸A similar effect may be induced by external electromagnetic interactions, which from a condensed-matter point of view are natural to consider. Recently, the effects of constant magnetic fields on the opening of a mass gap at the nodes of d -wave high-temperature superconductors have been considered in the experiments of Ref. [41]. Claims that this may induce, for strong enough fields, a change of state of the condensate into a parity-violating one, have been made [52]. Indeed, in the case of a constant external magnetic field, perpendicular to the spatial plane, one has an external source term violating parity and time-reversal symmetry. For strong enough source fields it is possible that a parity-violating condensate is magnetically induced. Such a phenomenon is at present a conjecture, which needs to be demonstrated analytically (via Schwinger-Dyson analysis) or on the lattice. We postpone such an issue for future investigations. We should mention, however, that recent preliminary lattice [50] or continuum [40] analyses, in the presence of an external field, showed that the magnetic field enhances the parity-conserving condensate.

tory experiments which might shed light to the physics of the early stages of our Universe. In the same spirit, the rich, and unconventional, structure of the high-temperature cuprates, depicted in Fig. 7, may also find interesting, and possibly new, applications to particle physics.

ACKNOWLEDGMENTS

It is a pleasure to acknowledge discussions with I. J. R. Aitchison, J. Betouras, C. P. Korthals-Altes, M. Teper, and A. Tsvelik. The work of N.E.M. and D. McN. was supported by the PPARC (UK). K.F. wishes to thank the TMR project FMRX-CT97-0122 for partial financial support, and the Department of Theoretical Physics of Oxford University for the hospitality during the last stages of this work.

APPENDIX A: RULES FOR MULTIPLE “MESON” PAIRING

When we come to calculate the meson pairs on a particular site there is a subtle complication if there are two pairs on the site, i.e., four Ψ 's and four $\bar{\Psi}$'s. Let us take as an example the function $[\text{tr}(\bar{A}_{i,\mu} A_{i,\mu})]^4$ which lies on the link $(i, i+\mu)$. Expanded out this gives

$$\begin{aligned} & [\bar{\Psi}_i^{b,\alpha} (-\gamma_\mu)^{\alpha\beta} \Psi_{i+\mu}^{a,\beta} \bar{\Psi}_{i+\mu}^{a,\gamma} (\gamma_\mu)^{\gamma\delta} \Psi_i^{b,\delta}] \\ & \times [\bar{\Psi}_i^{d,\epsilon} (-\gamma_\mu)^{\epsilon\zeta} \Psi_{i+\mu}^{c,\zeta} \bar{\Psi}_{i+\mu}^{c,\theta} (\gamma_\mu)^{\theta\eta} \Psi_i^{d,\eta}] \\ & \times [\bar{\Psi}_i^{f,\kappa} (-\gamma_\mu)^{\kappa\lambda} \Psi_{i+\mu}^{e,\lambda} \bar{\Psi}_{i+\mu}^{e,\pi} (\gamma_\mu)^{\pi\rho} \Psi_i^{f,\rho}] \\ & \times [\bar{\Psi}_i^{h,\sigma} (-\gamma_\mu)^{\sigma\tau} \Psi_{i+\mu}^{g,\tau} \bar{\Psi}_{i+\mu}^{g,\phi} (\gamma_\mu)^{\phi\chi} \Psi_i^{h,\chi}]. \end{aligned} \quad (\text{A1})$$

Before, when we just had a term which produced one pair of mesons on each site there was only one unique way of combining the $(\Psi\bar{\Psi})$ at that site to make the meson. However, now, as we see, there are three ways at each site. Writing down the fields at site i

$$\Psi_i^{b,\delta} \bar{\Psi}_i^{b,\alpha} \Psi_i^{d,\eta} \bar{\Psi}_i^{d,\epsilon} \Psi_i^{f,\rho} \bar{\Psi}_i^{f,\kappa} \Psi_i^{h,\chi} \bar{\Psi}_i^{h,\sigma} \quad (\text{A2})$$

these can be combined into pairs in three ways:

$$\Psi_i^{b,\delta} \bar{\Psi}_i^{d,\epsilon} \Psi_i^{d,\eta} \bar{\Psi}_i^{b,\alpha} \times \Psi_i^{f,\rho} \bar{\Psi}_i^{h,\sigma} \Psi_i^{h,\chi} \bar{\Psi}_i^{f,\kappa},$$

or

$$\Psi_i^{b,\delta} \bar{\Psi}_i^{h,\sigma} \Psi_i^{h,\chi} \bar{\Psi}_i^{b,\alpha} \times \Psi_i^{f,\rho} \bar{\Psi}_i^{d,\epsilon} \Psi_i^{d,\eta} \bar{\Psi}_i^{f,\kappa},$$

or

$$\Psi_i^{b,\delta} \bar{\Psi}_i^{f,\kappa} \Psi_i^{f,\rho} \bar{\Psi}_i^{b,\alpha} \times \Psi_i^{h,\chi} \bar{\Psi}_i^{d,\epsilon} \Psi_i^{d,\eta} \bar{\Psi}_i^{h,\sigma}. \quad (\text{A3})$$

When faced with a choice of three possible meson states, we must assume that each is likely to happen with equal probability (in a sense they can be seen as quantum states with equal energy) and so we write the final combination state at site i as

$$\begin{aligned} & \frac{1}{3} \Psi_i^{b,\delta} \bar{\Psi}_i^{d,\epsilon} \Psi_i^{d,\eta} \bar{\Psi}_i^{b,\alpha} \Psi_i^{f,\rho} \bar{\Psi}_i^{h,\sigma} \Psi_i^{h,\chi} \bar{\Psi}_i^{f,\kappa} \\ & + \frac{1}{3} \Psi_i^{b,\delta} \bar{\Psi}_i^{h,\sigma} \Psi_i^{h,\chi} \bar{\Psi}_i^{b,\alpha} \Psi_i^{f,\rho} \bar{\Psi}_i^{d,\epsilon} \Psi_i^{d,\eta} \bar{\Psi}_i^{f,\kappa} \\ & + \frac{1}{3} \Psi_i^{b,\delta} \bar{\Psi}_i^{f,\kappa} \Psi_i^{f,\rho} \bar{\Psi}_i^{b,\alpha} \Psi_i^{h,\chi} \bar{\Psi}_i^{d,\epsilon} \Psi_i^{d,\eta} \bar{\Psi}_i^{h,\sigma} \end{aligned} \quad (\text{A4})$$

or

$$\begin{aligned} & \left\{ \frac{1}{3} \text{tr}_c [M_i^{\delta\epsilon} M_i^{\eta\alpha}] \text{tr}_c [M_i^{\rho\sigma} M_i^{\chi\kappa}] + \frac{1}{3} \text{tr}_c [M_i^{\delta\sigma} M_i^{\chi\alpha}] \right. \\ & \left. \times \text{tr}_c [M_i^{\rho\epsilon} M_i^{\eta\kappa}] + \frac{1}{3} \text{tr}_c [M_i^{\delta\kappa} M_i^{\rho\alpha}] \text{tr}_c [M_i^{\chi\epsilon} M_i^{\eta\sigma}] \right\}. \end{aligned} \quad (\text{A5})$$

This must be contracted with the gamma matrices on the link and then with the meson states on site $i+\mu$, calculated in the same way. This procedure must also be followed when the four $(\Psi\bar{\Psi})$ pairs on the site come from two functions on adjacent sides meeting at that site.

APPENDIX B: THE “MESON” JACOBIAN

In this appendix we shall calculate the Jacobian of the transformation from the fermion variables $\bar{\Psi}_{\alpha,a}, \Psi_{\alpha,a}$, to the meson variables $\mathcal{M}_{\alpha\beta}^{ab} \equiv \Psi_{\beta}^b \bar{\Psi}_{\alpha}^a$. This change of variables implies the following transformation in the path integral:

$$\prod_i \int d\bar{\Psi}_i d\Psi_i \rightarrow \prod_i \int dM_i. \quad (\text{B1})$$

We adapt the method outlined in Ref. [26]. Let our initial path integral be written

$$\begin{aligned} & \prod_i \int d\bar{\Psi}_i d\Psi_i e^{S_{\text{eff}}[M_i]} \\ & = \prod_i e^{S_{\text{eff}}[\delta/J]} \int d\bar{\Psi}_i d\Psi_i e^{\text{tr} JM_i}|_{J=0}, \end{aligned} \quad (\text{B2})$$

the above fermionic integral can be evaluated,

$$\begin{aligned} & \int d\bar{\Psi} d\Psi e^{\text{tr} JM} = \int d\bar{\Psi} d\Psi e^{\bar{\Psi} J \Psi} = \det J, \\ & \bar{\Psi} J \Psi = \bar{\Psi}^{\alpha a} J^{ab\alpha\beta} \Psi^{b\beta}, \end{aligned} \quad (\text{B3})$$

where $\det J$ means the product of the eigenvalues of J , which is a 2×2 matrix in two spaces. However, there is a problem defining exactly what we mean by the measure dM , since M lives in two spaces. However, if we instead regard M as a 4×4 matrix we can use some simple results from group integration [54,26] to define a measure. The following identity is true for a $U(4)$ group integral:

$$\int dU \frac{1}{\det RU} e^{\text{tr} J'RU} = \det J', \quad (\text{B4})$$

where R is any positive-definite Hermitian matrix. The matrix J' is chosen to be the equivalent matrix in 4×4 space to the J defined in Eq. (B2) which lived in two 2×2 spaces. But the determinant of both are the same, $\det J' = \det J$. It is then a simple matter of associating, in Eq. (B4), $dU \mapsto dM$ and $RU \mapsto M$ and we get

$$\int d\bar{\Psi} d\Psi e^{\text{tr} JM} = \int dM \frac{1}{\det M} e^{\text{tr} JM}, \quad (\text{B5})$$

and our path integral becomes

$$\prod_i \int dM_i e^{-\sum_i \ln \det M + S_{\text{eff}}}. \quad (\text{B6})$$

Our path integral dM_i over the 4×4 space which we have represented as a group integral, can be viewed as a multi-component generalization of a contour integral.

If M_i had been a complex number, which is the case of a $U(1)$ gauge theory with Kogut-Susskind lattice fermions, we would have had [26]

$$\int d\bar{\Psi} \Psi e^{\bar{\Psi} J \Psi} = J = \oint \frac{dz}{2\pi iz} \frac{e^{Jz}}{z}. \quad (\text{B7})$$

This contour integral can be evaluated by parametrizing $z = Re^{i\theta}$, which is of course a representation of the $U(1)$ group. In such a case, this property of the Jacobian, expressible in terms of contour Cauchy integrals, can be used to infer stability of the broken vacuum in strongly coupled gauge theories, despite the appearance of a local maximum in the potential. A detailed discussion may be found in Ref. [26], where we refer the reader for more details. Below we shall only concentrate to a description of the basic results, pertinent for our analysis in this work.

In our problem, M is a 4×4 matrix and thus has 16 degrees of freedom. These degrees of freedom are illustrated in the expansion of M (12) in terms of the ‘‘lengths’’ (the \mathcal{A} 's and \mathcal{F} 's) along the 16 ‘‘axes.’’ However, we were interested in symmetry breaking along just one of these ‘‘axes,’’ $\sigma_3 \cdot \mathbf{1}$, with a ‘‘length’’ given by the complex number \mathcal{A}_3 . So we can view the important part of the integral dM as being in the complex plane where the only degree of freedom is \mathcal{A}_3 . In this respect we have complexified the VEV of \mathcal{A}_3 in order to apply the contour integration. Eventually, the effective potential will be minimized for real $\langle \mathcal{A}_3 \rangle$. We have thus a standard contour integral as above Eq. (B7).

To make things clearer it is useful [26] to add an explicit chiral-symmetry-breaking fermion mass term, $\sum_i m \bar{\Psi}_i \sigma_3 \Psi_i$, to our Lagrangian. The VEV of $\mathcal{A}_3(i)$ can be written as [26]

$$\begin{aligned} \langle \mathcal{A}_3(i) \rangle &= U e^{i\varphi} \quad \text{even sites,} \\ \langle \mathcal{A}_3(i) \rangle &= U e^{-i\varphi} \quad \text{odd sites.} \end{aligned} \quad (\text{B8})$$

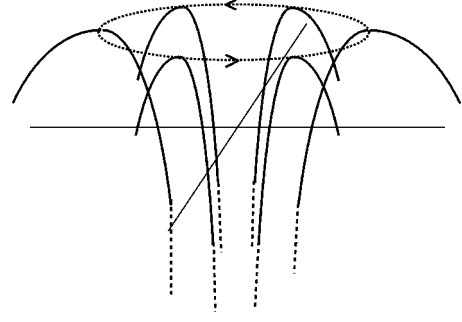


FIG. 10. Explanation on stability despite the existence of a local maximum in the effective potential.

The VEV of the mass term $\langle m \bar{\Psi}_i \sigma_3 \Psi_i \rangle$ is $m \langle \mathcal{A}_3(i) \rangle$ and so summed over even and odd sites will pick out the real part of the complex number:

$$\sum_i m \langle \mathcal{A}_3(i) \rangle = \sum_i \frac{1}{2} m U \cos \varphi. \quad (\text{B9})$$

Our effective potential now with the mass term is given in the form

$$V_{\text{eff}} \sim \frac{2}{3} \ln U^4 - P(U^4) - \frac{mU}{6} \cos \varphi, \quad (\text{B10})$$

where $P(U^4)$ represents the polynomial in U^4 which makes up the rest of V_{eff} , given in the text (43),(55). It is now clear how the apparent maximum at the stationary point is interpreted. Since the path integral is effectively a contour integral, we can choose our contour around the circle $|\langle \mathcal{A}_3(i) \rangle| = U$.

Then, the important parameter for minimizing V_{eff} is φ , and the minimum along the contour occurs at $\varphi=0$. The local maximum in V_{eff} lies along the radial direction U (see Fig. 10), which is irrelevant given that our variation of the potential is constrained to lie along the contour. As $m \rightarrow 0$, the minimum flattens and the whole contour becomes degenerate. By this argument, one will have a dynamically generated nonzero VEV for \mathcal{A}_3 , even in the absence of a bare mass term. Although this could equally be applied to any of the terms in the bilinear expansion of M_i , we know from the discussion of Vafa-Witten [25], briefly reviewed in Sec. II, that the parity-conserving mass \mathcal{A}_3 is energetically favored.

APPENDIX C: OUTLINE OF STRONG-COUPLING COMPUTATIONAL RULES

We want to calculate the following function on the plaquette:

$$\begin{aligned} J_p &= \left\{ \prod_{i,\mu \in p} \int dV_{i,\mu} I_0^{\text{tr}}(2\sqrt{y_{i,\mu}}) \text{tr} V_p \text{tr} V_p^\dagger \right\} \\ &\times \left\{ \prod_{i,\mu \in p} \int dV_{i,\mu} I_0^{\text{tr}}(2\sqrt{y_{i,\mu}}) \right\}^{-1}, \\ &= Z_p (Z_p^0)^{-1} \end{aligned} \quad (\text{C1})$$

with

$$I_0^{\text{tr}}(2\sqrt{y_{i,\mu}}) = 1 + y_{i,\mu} + \frac{y_{i,\mu}^2}{4} + \frac{y_{i,\mu}^3}{36} + \frac{y_{i,\mu}^4}{576},$$

$$y_{i,\mu} = \text{tr}(A_{i,\mu} V_{i,\mu}) \text{tr}(\bar{A}_{i,\mu} V_{i,\mu}^\dagger). \quad (\text{C2})$$

Our convention will be to label the sides of the plaquette 1,2,3,4 and the sites A,B,C,D . We need to perform the group integrals $\int dV_{i,\mu}$ on each side of the plaquette. In the case of Z_p^0 this will give a product of polynomials in $O(\bar{A}\bar{A})$ on each side (36):

$$Z_0 = \prod_{i,\mu \in p} \int dV_{i,\mu} I_0^{\text{tr}}(2\sqrt{y_{i,\mu}})$$

$$= \left(1 + \frac{1}{2}\text{tr}(A_1\bar{A}_1) + \dots\right) \left(1 + \frac{1}{2}\text{tr}(A_2\bar{A}_2) + \dots\right)$$

$$\times \left(1 + \frac{1}{2}\text{tr}(A_3\bar{A}_3) + \dots\right) \left(1 + \frac{1}{2}\text{tr}(A_4\bar{A}_4) + \dots\right). \quad (\text{C3})$$

Z_p will not be separable into products of simple link-polynomials because of the $\text{tr} V_p \text{tr} V_p^\dagger$ which connects the color indices of the links around the plaquette in a nontrivial way. For example, there could be a term such as $\text{tr}(A_1 A_2 A_3 A_4 \bar{A}_4 \bar{A}_3 \bar{A}_2 \bar{A}_1)$ in Z_p which would definitely be absent in Z_p^0 .

Z_p and Z_p^0 are both truncated due to the Grassmann fields $(\Psi\bar{\Psi})$ contained in the A, \bar{A} functions. So, e.g., a term such as $\text{tr}(A_1 \bar{A}_1)^4 \text{tr}(A_2 \bar{A}_2)$ will be immediately zero because there are too many fields at site B between sides 1 and 2. However, e.g., a term such as $\text{tr}(A_1 \bar{A}_1)^4 \text{tr}(A_3 \bar{A}_3)^4$ will survive.

A lot of the integrals in Z_p will turn out to be equal to their equivalent values in Z_p^0 . In fact the group integrals without at least a term of first order in $(\bar{A}\bar{A})$ on *every side* will just be equal to their zeroth order result. This is obvious if we consider, e.g.,

$$\int dV_1 dV_2 dV_3 dV_4 (\text{tr}(AV^\dagger) \text{tr}(\bar{A}\bar{V}))^2 \text{tr} V_p \text{tr} V_p^\dagger \quad \text{OR} \quad \text{O}(\bar{A}\bar{A})^4 \quad (\text{C4})$$

The diagram represents the plaquette with the clockwise flowing arrows being $\text{tr} V_p$ and the anticlockwise $\text{tr} V_p^\dagger$, (the reader should refer to Creutz [54] for a description of diagrammatic group integration). We do the group integral on one of the blank sides first. Following Creutz [54], this produces delta functions which contract with the other group matrices in $\text{tr} V_p \text{tr} V_p^\dagger$ all the way around the plaquette, removing them. This leaves the initial $[\text{tr}(AV^\dagger) \text{tr}(\bar{A}\bar{V})]^2$ without the $\text{tr} V_p \text{tr} V_p^\dagger$.

There are only nine terms in Z_p that do not have this simplification. They are the terms which have at least one power of $(\bar{A}\bar{A})$ on each side, i.e.,

$$\begin{aligned} & \text{O}(\bar{A}\bar{A}) \text{O}(\bar{A}\bar{A}) \text{O}(\bar{A}\bar{A}) \text{O}(\bar{A}\bar{A}) + \text{O}(\bar{A}\bar{A})^\dagger \text{O}(\bar{A}\bar{A})^\dagger \text{O}(\bar{A}\bar{A}) \text{O}(\bar{A}\bar{A}) \\ & + \text{O}(\bar{A}\bar{A})^\dagger \text{O}(\bar{A}\bar{A})^\dagger \text{O}(\bar{A}\bar{A}) \text{O}(\bar{A}\bar{A})^\dagger + \text{O}(\bar{A}\bar{A})^\dagger \text{O}(\bar{A}\bar{A})^\dagger \text{O}(\bar{A}\bar{A}) \text{O}(\bar{A}\bar{A})^\dagger \\ & + \text{O}(\bar{A}\bar{A})^\dagger \text{O}(\bar{A}\bar{A})^\dagger \text{O}(\bar{A}\bar{A})^\dagger \text{O}(\bar{A}\bar{A}) + \text{O}(\bar{A}\bar{A})^\dagger \text{O}(\bar{A}\bar{A})^\dagger \text{O}(\bar{A}\bar{A})^\dagger \text{O}(\bar{A}\bar{A})^\dagger \\ & + \text{O}(\bar{A}\bar{A})^\dagger \text{O}(\bar{A}\bar{A})^\dagger \text{O}(\bar{A}\bar{A})^\dagger \text{O}(\bar{A}\bar{A})^\dagger + \text{O}(\bar{A}\bar{A})^\dagger \text{O}(\bar{A}\bar{A})^\dagger \text{O}(\bar{A}\bar{A})^\dagger \text{O}(\bar{A}\bar{A})^\dagger \end{aligned} \quad (\text{C5})$$

The evaluation of these terms starts by splitting up the $\text{tr} V_p \text{tr} V_p^\dagger$ into $V_{ab} V_{cd}^\dagger$ pairs around the sides of the plaquette, working out the group integrals on each side (following Samuel [27]) and then “gluing” the sides together by contracting the spare color indices (ab, cd) .

As an example we give the explicit form for the first of the integrals in Eq. (C5)

$$\begin{aligned}
 & \int dV_1 dV_2 dV_3 dV_4 y_1 y_2 y_3 y_4 \operatorname{tr} V_p \operatorname{tr} V_p^\dagger \\
 &= \frac{41}{648} \operatorname{tr}(\bar{A}_1 A_1) \operatorname{tr}(\bar{A}_2 A_2) \operatorname{tr}(\bar{A}_3 A_3) \operatorname{tr}(\bar{A}_4 A_4) - \frac{1}{648} \{ \operatorname{tr}(\bar{A}_1 A_1) \operatorname{tr}(\bar{A}_2 A_2) \operatorname{tr}(A_3 A_4 \bar{A}_4 \bar{A}_3) + \operatorname{tr}(\bar{A}_2 A_2) \operatorname{tr}(\bar{A}_3 A_3) \operatorname{tr}(A_4 A_1 \bar{A}_1 \bar{A}_4) \\
 &+ \operatorname{tr}(\bar{A}_3 A_3) \operatorname{tr}(\bar{A}_4 A_4) \operatorname{tr}(A_1 A_2 \bar{A}_2 \bar{A}_1) + \operatorname{tr}(\bar{A}_4 A_4) \operatorname{tr}(\bar{A}_1 A_1) \operatorname{tr}(A_2 A_3 \bar{A}_3 \bar{A}_2) \} + \frac{1}{324} \{ \operatorname{tr}(\bar{A}_1 A_1) \operatorname{tr}(A_2 A_3 A_4 \bar{A}_4 \bar{A}_3 \bar{A}_2) \\
 &+ \operatorname{tr}(\bar{A}_2 A_2) \operatorname{tr}(A_3 A_4 A_1 \bar{A}_1 \bar{A}_4 \bar{A}_3) + \operatorname{tr}(\bar{A}_3 A_3) \operatorname{tr}(A_4 A_1 A_2 \bar{A}_2 \bar{A}_1 \bar{A}_4) + \operatorname{tr}(\bar{A}_4 A_4) \operatorname{tr}(A_1 A_2 A_3 \bar{A}_3 \bar{A}_2 \bar{A}_1) \} \\
 &+ \frac{1}{324} \{ \operatorname{tr}(A_1 A_2 \bar{A}_2 \bar{A}_1) \operatorname{tr}(A_3 A_4 \bar{A}_4 \bar{A}_3) + \operatorname{tr}(A_4 A_1 \bar{A}_1 \bar{A}_4) \operatorname{tr}(A_2 A_3 \bar{A}_3 \bar{A}_2) \} - \frac{1}{162} \{ \operatorname{tr}(A_1 A_2 A_3 A_4 \bar{A}_4 \bar{A}_3 \bar{A}_2 \bar{A}_1) \\
 &+ \operatorname{tr}(A_2 A_3 A_4 A_1 \bar{A}_1 \bar{A}_4 \bar{A}_3 \bar{A}_2) + \operatorname{tr}(A_3 A_4 A_1 A_2 \bar{A}_2 \bar{A}_1 \bar{A}_4 \bar{A}_3) + \operatorname{tr}(A_4 A_1 A_2 A_3 \bar{A}_3 \bar{A}_2 \bar{A}_1 \bar{A}_4) \} + \frac{1}{81} \operatorname{tr}(A_1 A_2 A_3 A_4) \operatorname{tr}(\bar{A}_4 \bar{A}_3 \bar{A}_2 \bar{A}_1).
 \end{aligned} \tag{C6}$$

It is obvious from Eq. (C6) above that the nine integrals are not separable into products of link functions. We rewrite $Z_p = Z_p^0 + Z_p'$ where Z_p' contains the above nine integrals minus the corresponding integrals in Z_p^0 (without the $\operatorname{tr} V_p \operatorname{tr} V_p^\dagger$). So $J_p = 1 + Z_p'(Z_p^0)^{-1}$. Expanding $(Z_p^0)^{-1}$ in powers of $O(A\bar{A})$,

$$\begin{aligned}
 (Z_p^0)^{-1} &= \prod_{i,\mu \in p} \left\{ 1 - \frac{1}{2} \operatorname{tr}(\bar{A}_{i,\mu} A_{i,\mu}) + \frac{1}{12} [\operatorname{tr}(\bar{A}_{i,\mu} A_{i,\mu})]^2 + \frac{1}{12} \operatorname{tr}[(\bar{A}_{i,\mu} A_{i,\mu})^2] \right. \\
 &\quad - \frac{1}{144} [\operatorname{tr}(\bar{A}_{i,\mu} A_{i,\mu})]^3 - \frac{1}{24} \operatorname{tr}[(\bar{A}_{i,\mu} A_{i,\mu})^3] + \frac{19}{1920} [\operatorname{tr}(\bar{A}_{i,\mu} A_{i,\mu})]^4 \\
 &\quad \left. - \frac{49}{2880} [\operatorname{tr}(\bar{A}_{i,\mu} A_{i,\mu})]^2 \operatorname{tr}[(\bar{A}_{i,\mu} A_{i,\mu})^2] + \frac{37}{5760} \operatorname{tr}[(\bar{A}_{i,\mu} A_{i,\mu})^2]^2 \right\},
 \end{aligned} \tag{C7}$$

where we have truncated up to order $O(A\bar{A})^4$

Looking at an example term in Z_p' , e.g.,

$$\int dV_1 dV_2 dV_3 dV_4 \frac{1}{64} (y_1)^2 (y_2)^2 y_3 (y_4)^2 \operatorname{tr} V_p \operatorname{tr} V_p^\dagger \quad \text{OR} \quad \begin{array}{c} \text{O}(\bar{A}\bar{A})^2 \\ \square \\ \text{O}(\bar{A}\bar{A})^2 \end{array} \quad \text{OR} \quad \begin{array}{c} \text{O}(\bar{A}\bar{A})^2 \\ \square \\ \text{O}(\bar{A}\bar{A})^2 \end{array} \quad \text{OR} \quad \begin{array}{c} \text{O}(\bar{A}\bar{A})^2 \\ \square \\ \text{O}(\bar{A}\bar{A})^2 \end{array} \quad \text{OR} \quad \begin{array}{c} \text{O}(\bar{A}\bar{A})^2 \\ \square \\ \text{O}(\bar{A}\bar{A})^2 \end{array}. \tag{C8}$$

When evaluated this will be an even more complicated function of $A_1, \bar{A}_1, A_2, \bar{A}_2, A_3, \bar{A}_3, A_4, \bar{A}_4$ than Eq. (C6). However, although it will have four pairs of $\Psi\bar{\Psi}$ at sites B and C (so two pairs of MM) it will have three pairs of $\Psi\bar{\Psi}$ at sites A and D which cannot be arranged solely into MM pairs. In order to give a nonzero contribution, this diagram will have to be multiplied by the factor $-\frac{1}{2} \operatorname{tr}(A_4 \bar{A}_4)$ coming from $(Z_p^0)^{-1}$. This will then give a diagram with $O(A\bar{A})^2$ on each side and all $\Psi\bar{\Psi}$ fields can be rearranged into $\operatorname{tr}(M_i M_i)$ form. So we must evaluate each of the nine diagrams in Eq. (C5) and then multiply each by whatever terms in $(Z_p^0)^{-1}$ (C7) will give a contribution containing pairs of $\Psi\bar{\Psi}$ at each site.

There will be only four ways of arranging the $O(A\bar{A})^n$ terms on each side of the plaquette to ensure that on each corner there are either two $\Psi\bar{\Psi}$ pairs or four $\Psi\bar{\Psi}$ pairs. These are shown below:

$$\begin{array}{c} \text{O}(\bar{A}\bar{A}) \\ \square \\ \text{O}(\bar{A}\bar{A}) \end{array} \quad \text{OR} \quad \begin{array}{c} \text{O}(\bar{A}\bar{A})^2 \\ \square \\ \text{O}(\bar{A}\bar{A})^2 \end{array} \quad \text{OR} \quad \begin{array}{c} \text{O}(\bar{A}\bar{A})^3 \\ \square \\ \text{O}(\bar{A}\bar{A})^3 \end{array} \quad \text{OR} \quad \begin{array}{c} \text{O}(\bar{A}\bar{A})^4 \\ \square \\ \text{O}(\bar{A}\bar{A})^4 \end{array}. \tag{C9}$$

Finally we describe the procedure for summing over all the delta functions which arise after substituting $\langle \text{tr} M_i^{\alpha\beta} M_i^{\gamma\delta} \rangle = 2U_i^2 \delta^{\alpha\beta} \delta^{\gamma\delta}$ at each site.

One term which will occur in $Z'_p(Z_p^0)^{-1}$ is

$$\begin{array}{c} O(\bar{A}\bar{A})^2 \\ \square \\ O(\bar{A}\bar{A})^2 \end{array}, \quad (C10)$$

where a simple possibility for $O(\bar{A}\bar{A})$ is $\text{tr}(A_{i,\mu} \bar{A}_{i,\mu})^2$. Of course there will be much more complicated terms of $O(\bar{A}\bar{A})^2$ where the A, \bar{A} are connected by color indices to other A, \bar{A} on adjacent sides, but the procedure will be the same:

$$\begin{aligned} [\text{tr}(\bar{A}_1 A_1)]^2 &= [\bar{\Psi}_A^{b,\alpha} (-\gamma_\mu)^{\alpha\beta} \Psi_B^{a,\beta} \bar{\Psi}_B^{\gamma} (\gamma_\mu)^{\gamma\delta} \Psi_A^{b,\delta}] \\ &\times [\bar{\Psi}_A^{d,\epsilon} (-\gamma_\mu)^{\epsilon\zeta} \Psi_B^{c,\zeta} \bar{\Psi}_B^{\theta} (\gamma_\mu)^{\theta\eta} \Psi_A^{d,\eta}], \end{aligned} \quad (C11)$$

and this can be rewritten

$$\begin{aligned} &\sim (\Psi_A^{b,\delta} \bar{\Psi}_A^{b,\alpha} \Psi_A^{d,\eta} \bar{\Psi}_A^{d,\epsilon}) (\gamma_\mu^{\alpha\beta} \gamma_\mu^{\gamma\delta} \gamma_\mu^{\epsilon\zeta} \gamma_\mu^{\theta\eta}) \\ &\times (\Psi_B^{a,\beta} \bar{\Psi}_B^{a,\gamma} \Psi_B^{c,\zeta} \bar{\Psi}_B^{c,\theta}), \end{aligned} \quad (C12)$$

or in a more abstract form

$$a^A \cdot X^{AB} \cdot a^B, \quad (C13)$$

where the center dot represents the contraction over the Dirac indices. So all around the plaquette we have $[\text{tr}(\bar{A}_1 A_1)]^2 [\text{tr}(\bar{A}_2 A_2)]^2 [\text{tr}(\bar{A}_3 A_3)]^2 [\text{tr}(\bar{A}_4 A_4)]^2$, written in this abstract form as

$$(a^A \cdot X^{AB} \cdot a^B) (a^B \cdot X^{BC} \cdot a^C) (a^C \cdot X^{CD} \cdot a^D) (a^D \cdot X^{DA} \cdot a^A) \quad (C14)$$

or

$$\text{Tr}[(a^A a^A) \cdot X^{AB} \cdot (a^B a^B) \cdot X^{BC} \cdot (a^C a^C) \cdot X^{CD} \cdot (a^D a^D) \cdot X^{DA}], \quad (C15)$$

where Tr is, at the moment, just indicating that all Dirac indices are being summed over. $(a^A a^A)$ now has eight Dirac indices, four of which it contracts with X^{AB} and four with X^{DA} .

The next step, is to rearrange the 4 $(\Psi_i, \bar{\Psi}_i)$ pairs in $(a^i a^i)$ into 2 meson pairs. As mentioned in Appendix A, this can be done in three, equally likely ways. The function at site B, $a^B a^B$ will be of the form

$$a^B a^B \sim \Psi_B^{a,\beta} \bar{\Psi}_B^{a,\gamma} \Psi_B^{c,\zeta} \bar{\Psi}_B^{c,\theta} \Psi_B^{f,\rho} \bar{\Psi}_B^{f,\kappa} \Psi_B^{h,\chi} \bar{\Psi}_B^{h,\sigma}, \quad (C16)$$

where $\Psi_B^{a,\beta} \bar{\Psi}_B^{a,\gamma} \Psi_B^{c,\zeta} \bar{\Psi}_B^{c,\theta}$ comes from side AB and $\Psi_B^{f,\rho} \bar{\Psi}_B^{f,\kappa} \Psi_B^{h,\chi} \bar{\Psi}_B^{h,\sigma}$ from side BC. We rewrite this as

$$\begin{aligned} &= \frac{1}{3} \Psi_B^{a,\beta} \bar{\Psi}_B^{c,\theta} \Psi_B^{c,\zeta} \bar{\Psi}_B^{a,\gamma} \Psi_B^{f,\rho} \bar{\Psi}_B^{h,\sigma} \Psi_B^{h,\chi} \bar{\Psi}_B^{f,\kappa} \\ &+ \frac{1}{3} \Psi_B^{a,\beta} \bar{\Psi}_B^{h,\sigma} \Psi_B^{h,\chi} \bar{\Psi}_B^{a,\gamma} \Psi_B^{f,\rho} \bar{\Psi}_B^{c,\theta} \Psi_B^{c,\zeta} \bar{\Psi}_B^{f,\kappa} \\ &+ \frac{1}{3} \Psi_B^{a,\beta} \bar{\Psi}_B^{f,\kappa} \Psi_B^{f,\rho} \bar{\Psi}_B^{a,\gamma} \Psi_B^{c,\zeta} \bar{\Psi}_B^{h,\sigma} \Psi_B^{h,\chi} \bar{\Psi}_B^{c,\theta}. \end{aligned} \quad (C17)$$

Now we substitute in $\langle M_i^{ab, \alpha\beta} \rangle = U_i \sigma_3^{ab} \delta^{\alpha\beta}$ to get

$$\frac{4}{3} U_B^4 \{ \delta^{\beta\theta} \delta^{\zeta\gamma} \delta^{\rho\sigma} \delta^{\chi\kappa} + \delta^{\beta\sigma} \delta^{\chi\gamma} \delta^{\rho\theta} \delta^{\zeta\kappa} + \delta^{\beta\kappa} \delta^{\rho\gamma} \delta^{\zeta\sigma} \delta^{\chi\theta} \}. \quad (C18)$$

So we have effectively replaced $(a^i a^i)$ with $\pm \frac{4}{3} U_i^4 \Delta^{\beta\theta\zeta\gamma\rho\sigma\chi\kappa}$, with Δ representing the sum of products of delta fns (the bit in $\{ \}$), which has 8 Dirac indices. The \pm above appears because when we rearrange the $(\Psi_i, \bar{\Psi}_i)$ we need to be careful about the anti-commuting Grassmann numbers.

Since each Dirac index has 2 possible values (it's a 2×2 representation of the Dirac algebra) and half the indices contract to the right and half to the left, we can re-represent the function Δ (a 2^8 tensor) with a 16×16 matrix. In (C18) the four indices $\beta\theta\zeta\gamma$ connect via four γ matrices to site A, and $\rho\sigma\chi\kappa$ connect via four γ matrices to site C. We can therefore replace each set of four indices (four pairs = sixteen combinations) with a single index taking 16 values. So $\Delta^{(\beta\theta\zeta\gamma)(\rho\sigma\chi\kappa)} = \Delta^{\Theta\Omega}$. The same goes for the functions X representing the four gamma matrices in (C15) and we merely need to calculate products of 16×16 matrices around the plaquette. The Tr in (C15) then becomes a matrix trace. Actually working out the matrix form for each product of delta functions then becomes a matter of bookkeeping. A helpful result is that, because of the symmetry of the problem and the even number of gamma matrices, we can actually replace the X 's with identity matrices.

We have outlined the procedure for working out one term, where all the corner functions were of the form $(a^i a^i)$ but the same goes for each term in $Z_p(Z_p^0)^{-1}$. In the case where there are spare color indices to contract at the corners we must do this first and then rearrange the $\Psi \bar{\Psi}$, but each corner will eventually be written similar to (C16).

For the other diagrams in Eq. (C9) there will not be four gamma matrices on the sides but rather two [for $O(\bar{A}\bar{A})$] or six [for $O(\bar{A}\bar{A})^3$] and these can be rewritten as 4×4 or 64×64 matrices, respectively. So the corner function will be a 4×4 matrix for a corner connecting two $O(\bar{A}\bar{A})$ sides, and for a corner connecting a $O(\bar{A}\bar{A})$ side and a $O(\bar{A}\bar{A})^3$ side a 4×64 matrix (with the transpose 64×4 for an adjacent corner). The general procedure, however, is identical in each case. Our computation is given in more detail in Ref. [38] and is summarized below.

(1) Work out the group integrals on each side, the result will be a sum of terms such as (C13). (2) Write the integral around the whole plaquette as a sum of terms each of the form (C15) contracting all spare color indices. (3) Replace

each corner functions with the sum of delta functions, being careful to keep track of \pm due to the anticommuting nature of $(\Psi_i, \bar{\Psi}_i)$. (4) Rewrite the Δ functions as 16×16 , 4×4 , or 4×64 matrices. (5) Trace over the matrices.

-
- [1] R. D. Pisarski, Phys. Rev. D **29**, 2423 (1984); T. W. Appelquist, M. Bowick, D. Karabali, and L. C. R. Wijewardhana, *ibid.* **33**, 3704 (1986); T. W. Appelquist, D. Nash, and L. C. R. Wijewardhana, Phys. Rev. Lett. **60**, 2575 (1988); I. J. R. Aitchison, N. E. Mavromatos, and D. Mc Neill, Phys. Lett. B **402**, 154 (1997).
- [2] K. Farakos, G. Koutsoumbas, and G. Zoupanos, Phys. Lett. B **249**, 101 (1990).
- [3] K. I. Kondo, T. Ebihara, T. Iizuka, and E. Tanaka, Nucl. Phys. **B434**, 85 (1995).
- [4] N. Dorey and N. E. Mavromatos, Phys. Lett. B **250**, 107 (1990); Nucl. Phys. **B386**, 614 (1992).
- [5] I. J. R. Aitchison and N. E. Mavromatos, Phys. Rev. B **39**, 6544 (1989).
- [6] K. Farakos and N. E. Mavromatos, Phys. Rev. B **57**, 3017 (1998).
- [7] I. Affleck, Z. Zou, T. Hsu, and P. W. Anderson, Phys. Rev. B **38**, 745 (1988).
- [8] P. W. Anderson, Science **235**, 1196 (1987).
- [9] R. B. Laughlin, Proceedings of the 4th Chia meeting on *Common Trends in Condensed Matter and Particle Physics*, Chia-Laguna, Italy, September, 1994 (unpublished).
- [10] J. Fröhlich and P. Marchetti, Phys. Rev. B **46**, 6535 (1992); J. Fröhlich, T. Kerler, and P. Marchetti, Nucl. Phys. **B374**, 511 (1992).
- [11] A. Kovner and B. Rosenstein, Mod. Phys. Lett. A **5**, 2661 (1990); Phys. Rev. B **42**, 4748 (1990); A. Kovner, B. Rosenstein, and D. Eliezer, Nucl. Phys. **B350**, 325 (1990).
- [12] J. Kosterlitz and D. Thouless, J. Phys. C **6**, 1181 (1973).
- [13] D. A. Bonn *et al.*, Phys. Rev. Lett. **68**, 2390 (1992); C. C. Tsuei *et al.*, *ibid.* **73**, 593 (1994); K. A. Moler *et al.*, *ibid.* **73**, 2744 (1994); J. R. Kirtley *et al.*, Nature (London) **373**, 225 (1995); D. Wollman *et al.*, Phys. Rev. Lett. **74**, 797 (1995).
- [14] A. M. Polyakov, *Gauge Fields and Strings* (Harwood, Chur, 1987); S. Deser and A. N. Redlich, Phys. Rev. Lett. **61**, 1541 (1989).
- [15] N. Dorey and N. E. Mavromatos, Phys. Rev. B **44**, 5286 (1991).
- [16] C. Burden and A. N. Burkitt, Europhys. Lett. **3**, 545 (1987).
- [17] I. Affleck and J. B. Marston, Phys. Rev. B **37**, 3774 (1988); **39**, 11 538 (1989).
- [18] R. Shankar, Phys. Rev. Lett. **63**, 203 (1989); Nucl. Phys. **B330**, 433 (1990).
- [19] I. Affleck, J. Harvey, and E. Witten, Nucl. Phys. **B206**, 413 (1982).
- [20] A. Loeser *et al.*, Science **273**, 325 (1996); H. Ding *et al.*, Nature (London) **382**, (1996); B. Batlogg *et al.*, Physica C **235-240**, 130 (1994); C. C. Homes *et al.*, Phys. Rev. Lett. **71**, 1645 (1993); A. V. Puchkov *et al.*, *ibid.* **77**, 3212 (1996).
- [21] K. Farakos, G. Koutsoumbas, and N. E. Mavromatos, cond-mat/9805402.
- [22] P. A. Marchetti, Z.-B. Su, and Lu Yu, cond-mat/9709109; cond-mat/9805191.
- [23] L. Balents, M. Fisher, and C. Nayak, cond-mat/9803086.
- [24] G. Volovik, talk at the *Workshop on Low Dimensional Fermi-liquid Systems*, Hamamatsu, Japan, October, 1997, cond-mat/9711031.
- [25] C. Vafa and E. Witten, Commun. Math. Phys. **95**, 257 (1984).
- [26] N. Kawamoto and J. Smit, Nucl. Phys. **B192**, 100 (1981).
- [27] S. Samuel, J. Math. Phys. **21**, 2695 (1980).
- [28] G. A. Diamandis, B. C. Georgalas, and N. E. Mavromatos, Mod. Phys. Lett. A **13**, 387 (1998).
- [29] K. Farakos and N. E. Mavromatos, Mod. Phys. Lett. A **13**, 1019 (1998).
- [30] P. Maris, Phys. Rev. D **54**, 4049 (1996).
- [31] S. Sharpe and R. Singleton, Jr, Phys. Rev. D **58**, 074501 (1998).
- [32] K. Bitar, U. Heller, and R. Narayanan, Phys. Lett. B **418**, 167 (1998).
- [33] T. Banks and A. Casher, Nucl. Phys. **B169**, 103 (1980).
- [34] S. Aoki, Phys. Rev. D **30**, 2653 (1984).
- [35] K. Farakos and G. Koutsoumbas, Phys. Lett. B **178**, 260 (1986).
- [36] M. Abramowitz and I. Stegun, *Handbook of Mathematical Functions* (Dover, New York, 1965).
- [37] E. Dagotto, A. Kocic, and J. B. Kogut, Phys. Rev. Lett. **62**, 1083 (1989); Nucl. Phys. **B334**, 279 (1990).
- [38] D. McNeill, Ph.D. dissertation, Oxford University, 1998.
- [39] N. Dorey, D. Tong, and S. Vandoren, J. High Energy Phys. **04**, 005 (1998).
- [40] K. Farakos and N. E. Mavromatos, Int. J. Mod. Phys. B **12**, 809 (1998).
- [41] K. Krishana *et al.*, Science **277**, 83 (1997).
- [42] I. J. R. Aitchison and N. E. Mavromatos, Phys. Rev. B **53**, 9321 (1996); I. J. R. Aitchison, G. Amelino-Camelia, M. Klein-Kreisler, N. E. Mavromatos, and D. Mc Neill, *ibid.* **56**, 2836 (1997).
- [43] R. Shankar, Rev. Mod. Phys. **66**, 129 (1994); J. Polchinski, *TASI Lectures 1992*, Boulder Colorado, hep-th/9210046.
- [44] A. M. Polyakov, *Gauge Fields and Strings* [14]; S. Deser and A. N. Redlich, Phys. Rev. Lett. **61**, 1541 (1989); B. Rosenstein and A. Kovner, Nucl. Phys. **B346**, 576 (1990).
- [45] N. E. Mavromatos and M. Ruiz-Altaba, Phys. Lett. A **142**, 419 (1989).
- [46] P. B. Wiegmann, Phys. Rev. Lett. **60**, 821 (1988); S. Sarkar, J. Phys. A **23**, L409 (1990); **24**, 1137 (1991); F. H. L. Essler, V. A. Korepin, and K. Schoutens, Phys. Rev. Lett. **68**, 2960 (1992); A. Lerda and S. Sciuto, Nucl. Phys. **B410**, 577 (1993).

- [47] G. Semenoff and L. C. R. Wijerwardhana, Phys. Rev. Lett. **64**, 2633 (1989).
- [48] A. Leggett, talk at Oxford, 1998 (unpublished).
- [49] B. Rosenstein, B. J. Warr, and S. H. Park, Phys. Rev. Lett. **62**, 1433 (1989); G. Gat, A. Kovner, B. Rosenstein, and B. J. Warr, Phys. Lett. B **240**, 158 (1990).
- [50] K. Farakos, G. Koutsoumbas, and N. E. Mavromatos, Phys. Lett. B **431**, 147 (1998).
- [51] G. Semenoff, I. A. Shovkovy, and R. Wijerwardhana, Mod. Phys. Lett. A **13**, 1143 (1998).
- [52] R. B. Laughlin, cond-mat/9709004.
- [53] J. Tranquada *et al.*, Nature (London) **375**, 561 (1995); Phys. Rev. B **54**, 7489 (1996); O. Zachar, S. A. Kivelson, and V. J. Emery, cond-mat/9702055, and references therein.
- [54] Michael Creutz, *Quarks, Gluons and Lattices* (Cambridge University Press, Cambridge, England, 1983).